Am J Transl Res 2020;12(5):1614-1639
www.ajtr.org /ISSN:1943-8141/AJTR0103714

Original Article

Kinesin family members KIF2C/4A/10/11/14/18B/20A/23 predict poor prognosis and promote cell proliferation in hepatocellular carcinoma

Xishan Li[1,2*], Weimei Huang[1*], Wenbin Huang[1], Ting Wei[1], Weiliang Zhu[1], Guodong Chen[2], Jian Zhang[1]

[1]Department of Oncology, Zhujiang Hospital, Southern Medical University, 253 Industrial Avenue, Guangzhou 510282, China; [2]Department of Interventional Radiology, Guangzhou First People's Hospital, The Second Affiliated Hospital of South China University of Technology, No. 1 Panfu Road, Guangzhou 510180, China. [*]Equal contributors.

Received October 18, 2019; Accepted April 22, 2020; Epub May 15, 2020; Published May 30, 2020

Abstract: Kinesin superfamily proteins (KIFs) comprise a family of molecular motors that transport membranous organelles and protein complexes in a microtubule- and ATP-dependent manner, with multiple roles in cancers. Little is known about the function of KIFs in hepatocellular carcinoma (HCC). Here, we investigate the roles of KIFs in the prognosis and progression of HCC. Upregulation of eight KIFs (KIF2C, KIF4A, KIF10, KIF11, KIF14, KIF18B, KIF20A, and KIF23) was found to be significantly associated with the tumor stage and pathological tumor grade of HCC patients. Additionally, a high expression of these eight KIFs was significantly associated with shorter overall survival (OS) and disease-free survival (DFS) in patients with HCC. Cox regression analysis showed the mRNA expression levels of these eight KIF members to be independent prognostic factors for worse outcomes in HCC. Moreover, a risk score model based on the mRNA levels of the eight KIF members effectively predicted the OS rate of patients with HCC. Additional experiments revealed that downregulation of each of the eight KIFs effectively decreased the proliferation and increased the G1 arrest of liver cancer cells in vitro. Taken together, these results indicate that KIF2C/4A/10/11/14/18B/20A/23 may serve as prognostic biomarkers for survival and potential therapeutic targets in HCC patients.

Keywords: Hepatocellular carcinoma, KIFs, prognosis, proliferation, migration, cell cycle

Introduction

Liver cancer is the second-ranked tumor-related cause of death worldwide, and hepatocellular carcinoma (HCC) accounts for 75%-85% of all primary liver tumors [1]. Despite the fact that the proportion of HCC cases diagnosed at an early stage has increased from 27% between 1992 and 1999 to 44% between 2006 and 2012 due to improved diagnosis and documentation of tumor stage, the 5-year survival rate of HCC is still less than 35% [2]. Therefore, a better understanding of the underlying pathogenesis and etiology of HCC is crucial for improving the early diagnosis and treatment of HCC.

Intervention in the process of cell division by disrupting the formation of mitotic spindles has been shown to be effective in anticancer therapy [3]. Microtubule (MT)-targeting agents disrupt MT dynamics, inducing prolonged mitotic arrest and eventually leading to cell death; examples of such agents include paclitaxel and docetaxel, which are applied in tumor treatment [4]. Kinesin superfamily proteins (KIFs) are a family of molecular motors that travel unidirectionally along MT tracks and play many roles in intracellular transport or cell division [5]. KIFs have been shown to be involved in the transport of organelles, protein complexes and mRNAs and to participate in chromosomal and spindle movements during mitosis and meiosis [6-9]. There are a total of 45 KIFs in eukaryotic cells [6]. KIFs are grouped into 14 subfamilies based molecular structure, and they all possess a highly conserved motor domain that provides motor binding to MTs [10]. Recent studies have demonstrated that kinesins might act as oncogenes in several cancer types [5, 11].

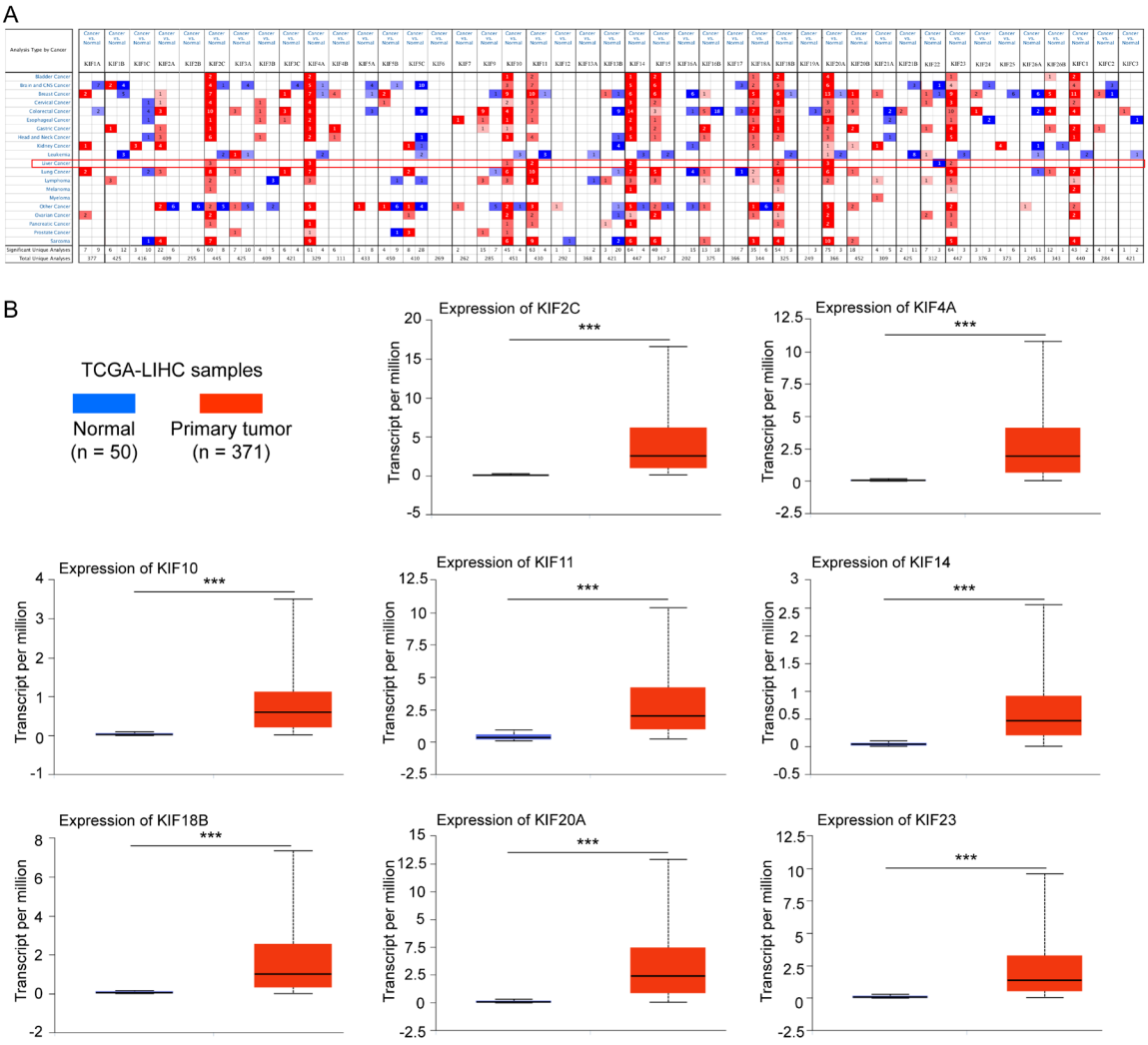

Figure 1. A. Transcriptional expression of KIFs in 20 different types of cancer (ONCOMINE database). Differences in transcriptional expression were compared by Student's t test. The parameters to determine the cut-off value were as follows: *p* value: 0.0001; fold change: 2; gene rank: 10%; and data type: mRNA. B. mRNA expression of distinct KIF superfamily members in HCC tissues and adjacent normal liver tissues (UALCAN). Differences in mRNA expression were compared by Student's t test. ***P < 0.001.

For example, KIFC3/C1/1A/5A were found to mediate docetaxel resistance in breast cancer cell lines [12]. Several inhibitors that specifically target certain kinesins have been used in clinical trial research, such as the Eg5 (KIF11) reagent AZD4877 and CENPE (KIF10) inhibitor GSK923295 [13, 14]. In addition, recent studies have reported that KIF20B inhibition enhances the toxicity of chemotherapeutic drugs in HCC [15, 16]. However, targeting a single KIF member is often insufficient to achieve ideal clinical outcomes for a number of solid tumors [17-19]. Therefore, a comprehensive study of different kinesin family members in HCC will help in our understanding of the molecular mechanisms involved in the development of HCC and reveal new prognostic and therapeutic targets for this cancer.

In the present study, we focused on eight distinct KIFs involved in the development and progression of HCC by evaluating the expression of different KIF family members and their relationships with clinical parameters in HCC patients. Furthermore, we analyzed the predicted functions and pathways that are affected when the eight KIF members are dysregulated in HCC. Our in vitro experiments confirmed that downregulation of the eight distinct KIFs effectively inhibits the proliferation of HCC cells by increasing G1 phase arrest, providing evidence that distinct KIFs might serve

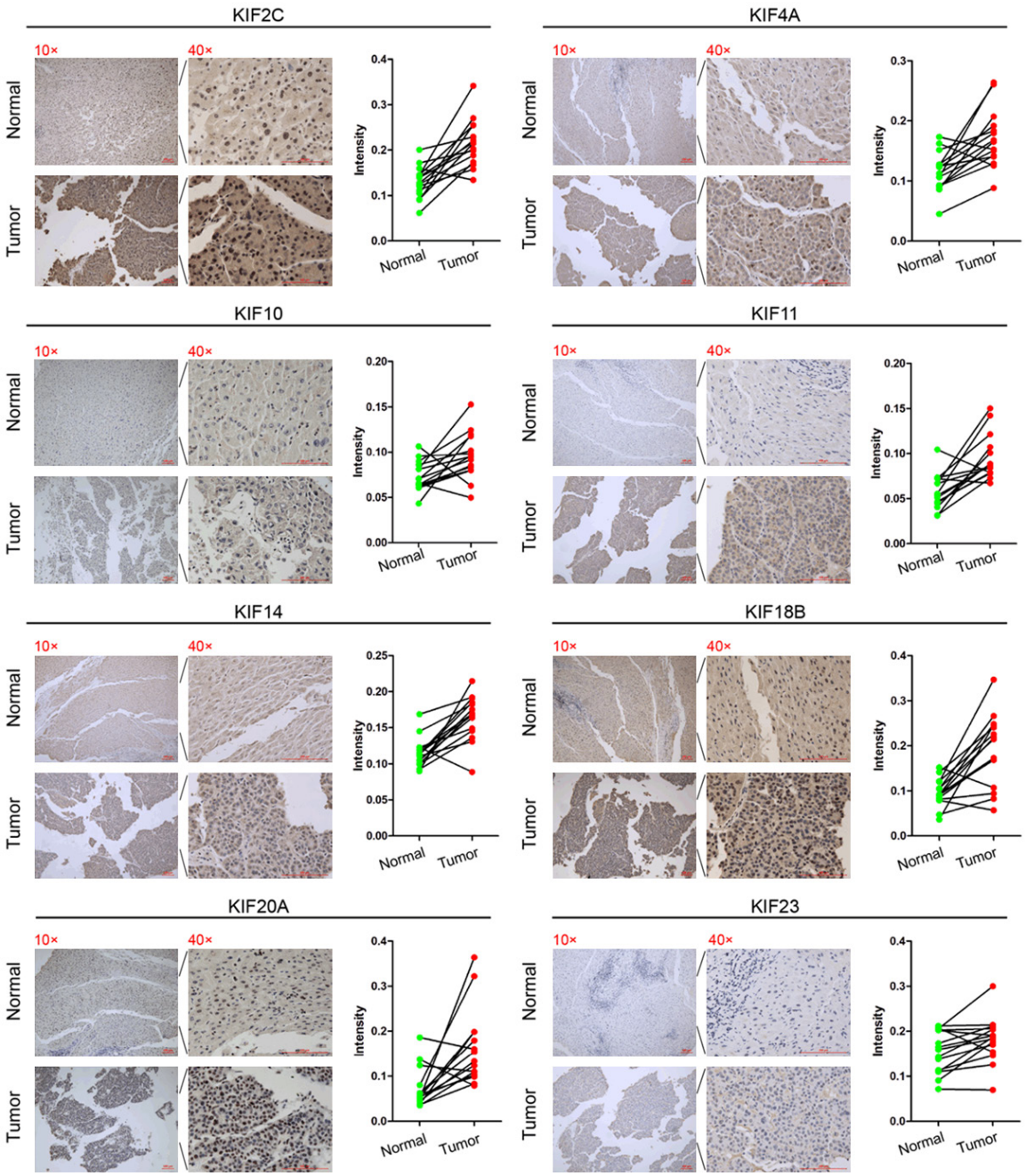

Figure 2. Representative immunohistochemistry images and protein intensity of distinct KIF members in the HCC tissues and corresponding normal liver tissues of 15 patients. The intensity of staining was measured by Image-Pro Plus 6.0 software. The protein levels of 8 distinct KIFs are higher in tumor tissues than that in corresponding normal liver tissues.

as novel prognostic biomarkers and therapeutic targets for HCC.

Materials and methods

Tissue specimens and ethics statement

Tissue samples were obtained from consecutive patients who underwent surgery as part of their clinical care at the Zhujiang Hospital of Southern Medical University. The study was approved by the institutional review board at Southern Medical University. Informed and signed consent was obtained from all patients at the time of surgery for the use of their tissue. The vast majority of the data for this study were obtained from several public online

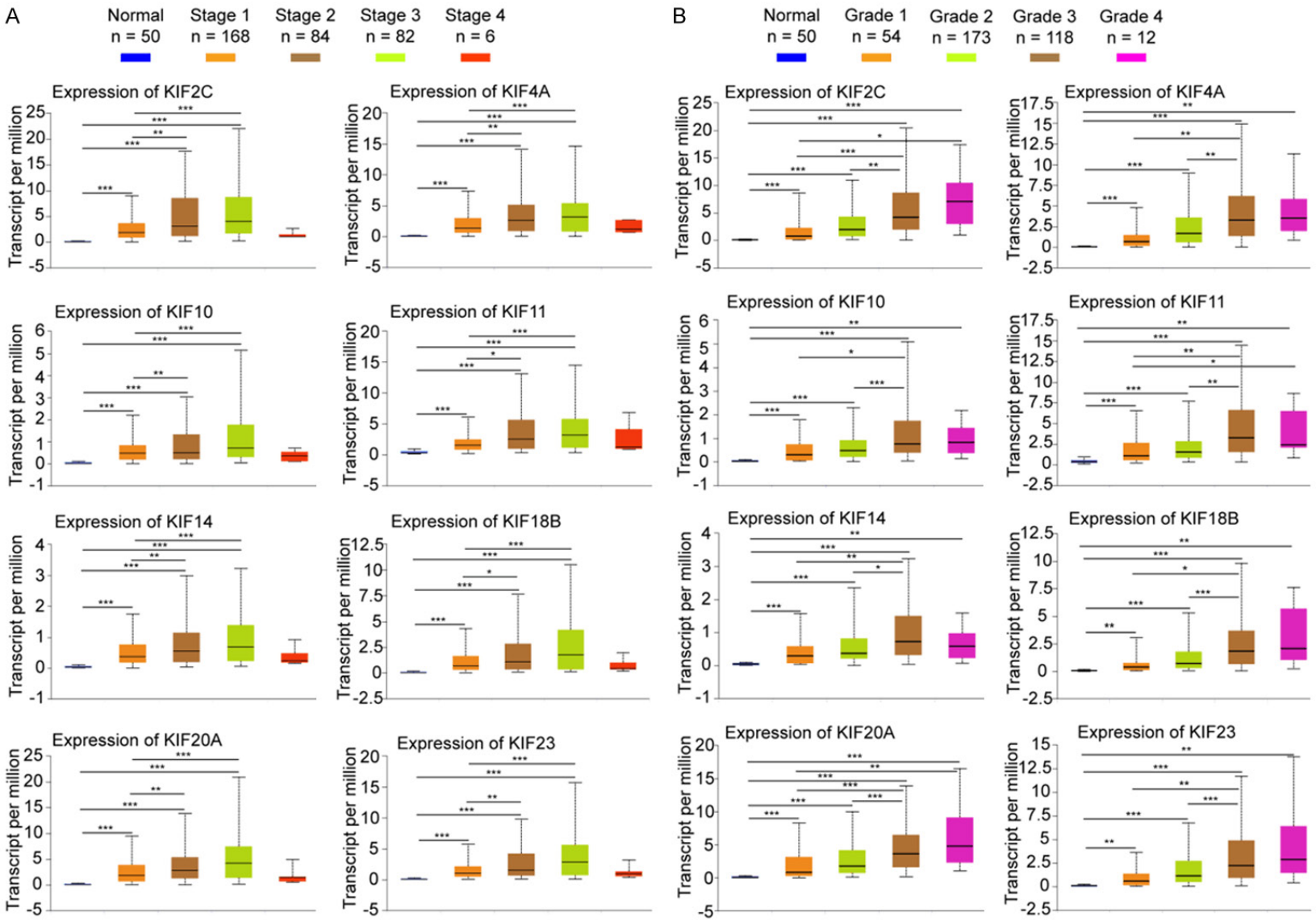

Figure 3. Association of the mRNA expression of distinct KIF superfamily members with tumor stages and grades of HCC patients. Differences in mRNA expression were compared by one-way ANOVA.

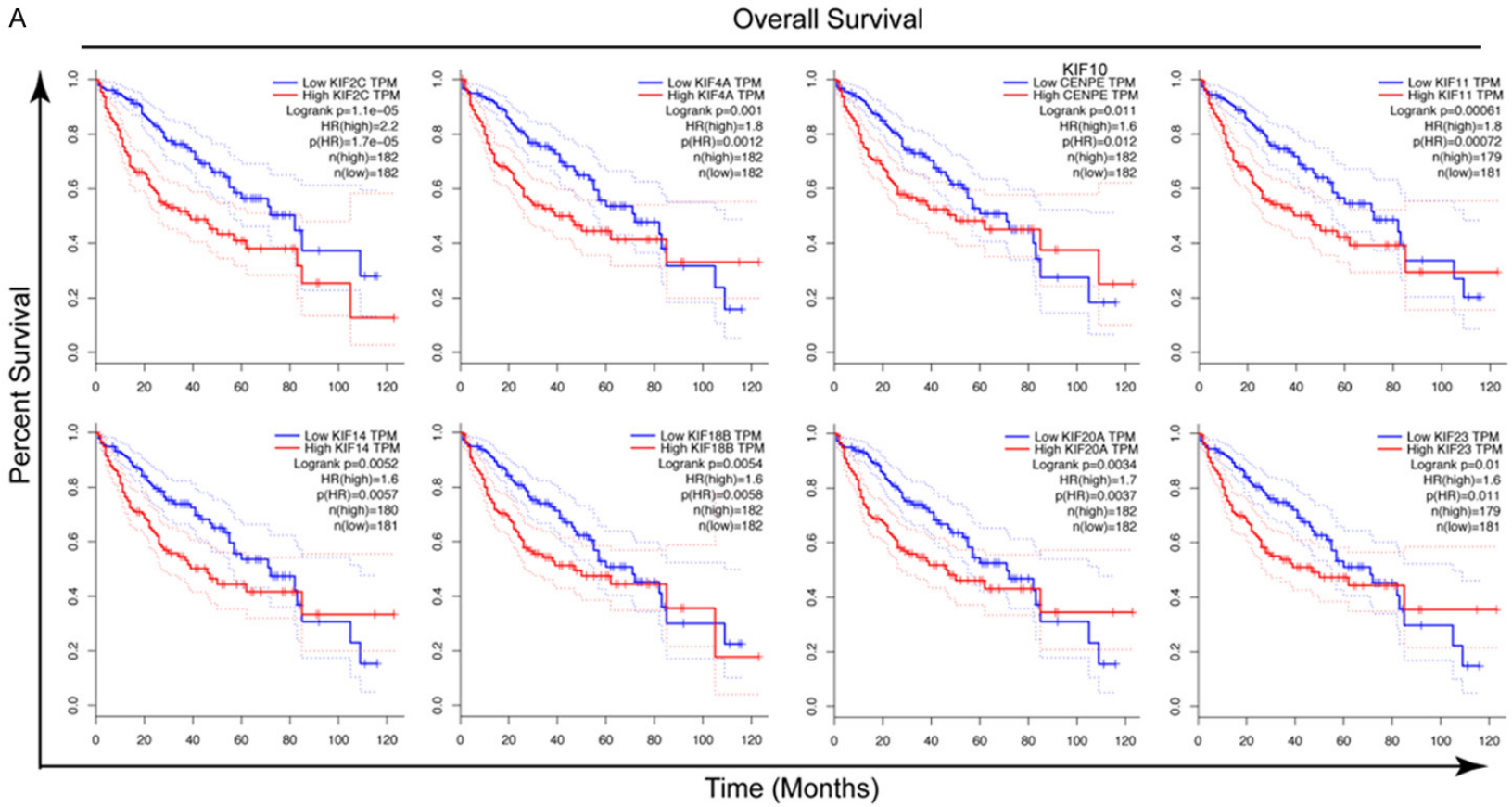
A
Overall Survival
Percent Survival
Time (Months)
Low KIF2C TPM
High KIF2C TPM
Logrank p=1.1e−05
HR(high)=2.2
p(HR)=1.7e−05
n(high)=182
n(low)=182
Low KIF4A TPM
High KIF4A TPM
Logrank p=0.001
HR(high)=1.8
p(HR)=0.0012
n(high)=182
n(low)=182
KIF10
Low CENPE TPM
High CENPE TPM
Logrank p=0.011
HR(high)=1.6
p(HR)=0.012
n(high)=182
n(low)=182
Low KIF11 TPM
High KIF11 TPM
Logrank p=0.00061
HR(high)=1.8
p(HR)=0.00072
n(high)=179
n(low)=181
Low KIF14 TPM
High KIF14 TPM
Logrank p=0.0052
HR(high)=1.6
p(HR)=0.0057
n(high)=180
n(low)=181
Low KIF18B TPM
High KIF18B TPM
Logrank p=0.0054
HR(high)=1.6
p(HR)=0.0058
n(high)=182
n(low)=182
Low KIF20A TPM
High KIF20A TPM
Logrank p=0.0034
HR(high)=1.7
p(HR)=0.0037
n(high)=182
n(low)=182
Low KIF23 TPM
High KIF23 TPM
Logrank p=0.01
HR(high)=1.6
p(HR)=0.011
n(high)=179
n(low)=181

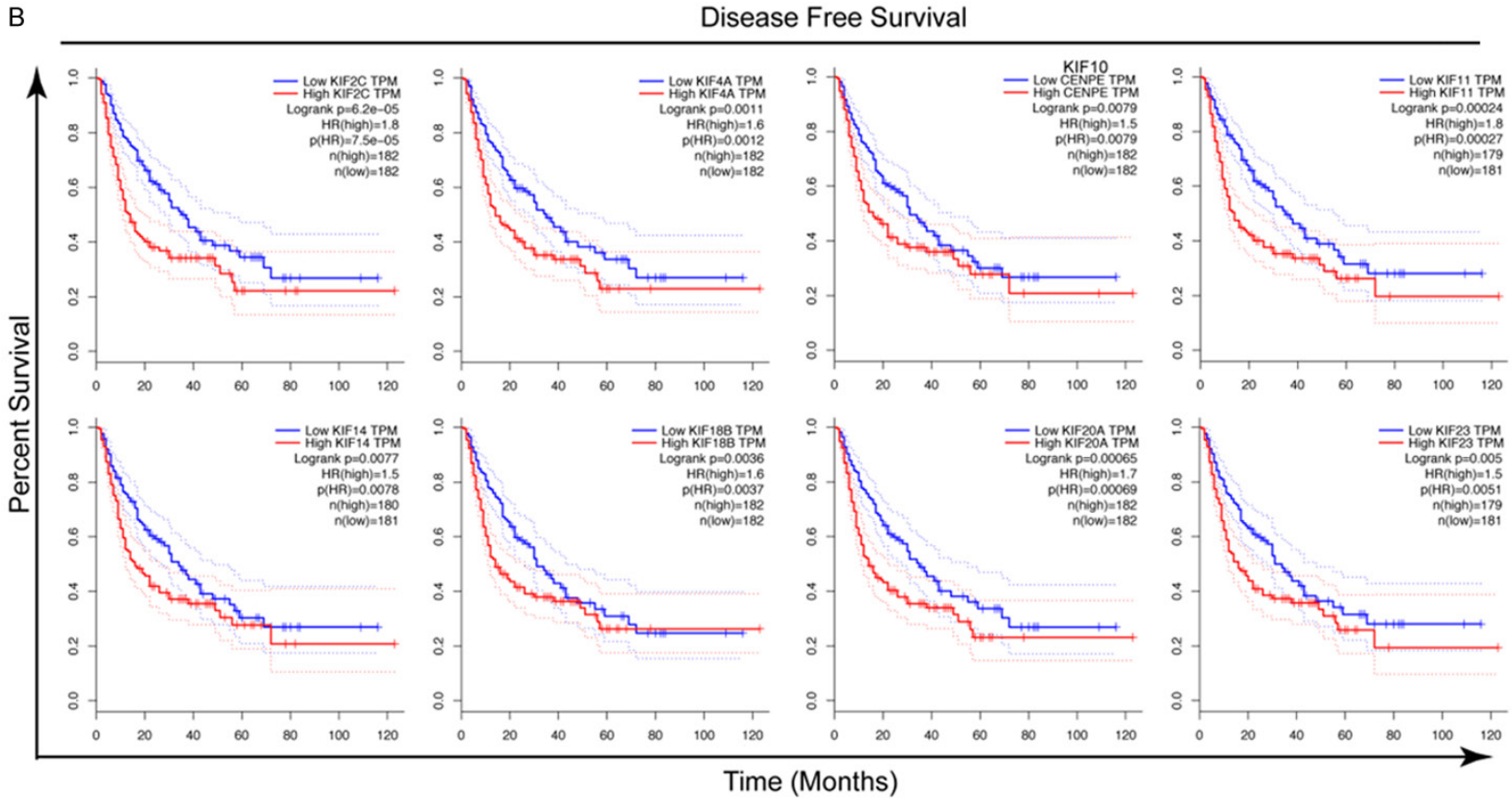

Figure 4. Prognostic value of the mRNA expression of distinct KIF family members in liver cancer patients (Kaplan-Meier plotter). A higher mRNA expression level of distinct KIF members was associated with poorer OS (A) and DFS (B) in liver cancer patients. Comparison of survival curves was carried out by using the log rank test.

databases, which confirmed that all written informed consent had already been obtained.

ONCOMINE database

ONCOMINE (www.oncomine.org) is a cancer microarray database and web-based data mining platform aimed at facilitating discovery based on genome-wide expression analyses [20]. In our present study, meta-analyses of distinct KIF superfamily members in 20 different tumor tissues and corresponding normal tissues were obtained from the ONCOMINE database. Student's t test was used to compare differences in the transcript levels of KIF members. The criteria for analysis were as follows: *p* value: 0.01; fold change: 2.0; gene rank: 10%; and data type: mRNA.

UALCAN

UALCAN (http://ualcan.path.uab.edu/) is an easy-to-use, interactive web portal for performing in-depth analyses of TCGA gene expression data that uses TCGA-level RNA-seq and clinical data from 31 cancer types [21]. Our study used the UALCAN online database to determine the differential expression of the eight KIF superfamily members in liver cancer and corresponding adjacent tissues. The number of normal tissues was 50, and the number of primary tumor tissues was 371. *** represents a *p* value of less than 0.001 based on Student's t test.

Human protein atlas

The Human Protein Atlas (www.proteinatlas.org) provides tissue and cell distribution information for all 24,000 human proteins through free public enquiries. We obtained immunohistochemical images of KIF superfamily members in normal tissues and liver cancer tissues for this study.

TCGA

TCGA is a landmark cancer genomics program that has molecularly characterized over 20,000 primary cancer and matched normal samples spanning 33 cancer types [22]. mRNA expression levels of KIFs in 371 HCC patients were downloaded. Complete follow-up information was available for 364 of the 371 patients; the data for the 364 patients were examined in our follow-up analysis.

cBioPortal

cBioPortal for Cancer Genomics is an open-source resource for the interactive exploration of multiple cancer genomics datasets. Genomic data types integrated by cBioPortal include somatic mutations, DNA copy-number alterations (CNAs), mRNA and microRNA (miRNA) expression, DNA methylation, protein abundance, and phosphoprotein abundance [23]. We used the cBioPortal platform to obtain gene expression matrices derived from TCGA to simplify our data analysis steps.

ICGC

ICGC (https://icgc.org/) was established to launch and coordinate a large number of research projects sharing a common goal of unraveling the genomic changes present in many forms of cancer that contribute to the disease burden in individuals worldwide. We obtained patient follow-up information and the gene expression matrix of the LIRI-JP project from ICGC, combined the gene symbol and gene expression matrix in Perl, and used this project as a validation set for our eight-KIF gene signature risk model.

KEGG analysis and oncogenic signature analysis

GSEA was employed to assess the distribution of genes in a predefined gene set in a phenotypic-ordered gene table to determine its contributions to phenotype [24]. Based on the GSEA platform, the functions of the eight KIF superfamily members were analyzed by KEGG and oncogenic signature enrichment to identify cancer-related signaling pathways and molecules associated with the KIF superfamily in HCC.

Development and validation of the prognostic signature

As shown in **Figure 5A**, TCGA-LIHC was used as the training set (366 samples), and ICGC LIRI-JP was used as the validation set (232 samples). A risk score was calculated by considering expression of the eight KIF genes and the correlation coefficient based on the dataset TCGA-LIHC. All patients were divided into different groups (high-risk group or low-risk group) according to the median of the risk score. Kaplan-Meier analysis was performed

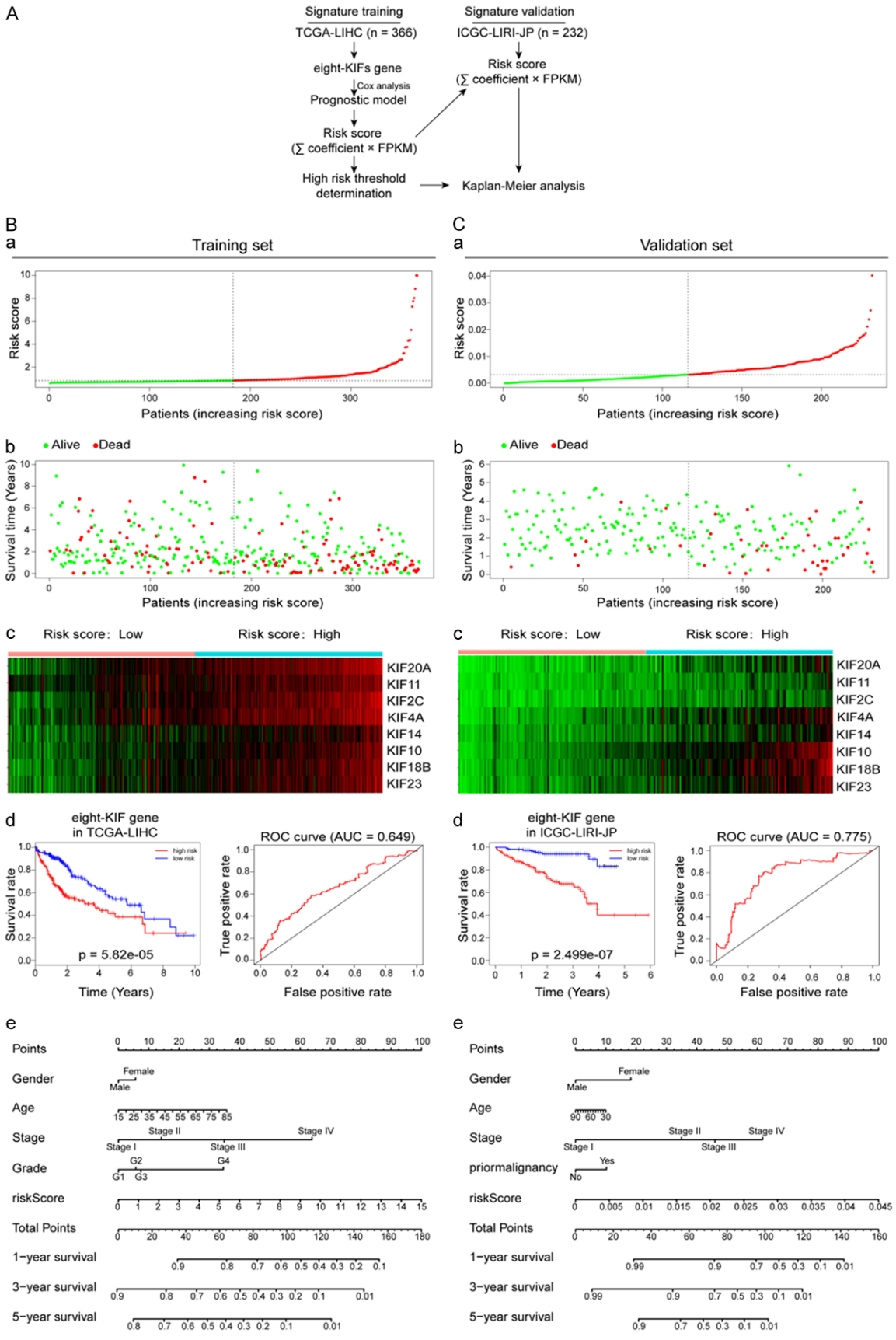
A
Signature training
TCGA-LIHC (n = 366)
eight-KIFs gene
Cox analysis
Prognostic model
Risk score
(∑ coefficient × FPKM)
High risk threshold determination
Signature validation
ICGC-LIRI-JP (n = 232)
Risk score
(∑ coefficient × FPKM)
Kaplan-Meier analysis
B
a
Training set
Risk score
Patients (increasing risk score)
b
Alive
Dead
Survival time (Years)
Patients (increasing risk score)
c
Risk score: Low
Risk score: High
KIF20A
KIF11
KIF2C
KIF4A
KIF14
KIF10
KIF18B
KIF23
d
eight-KIF gene in TCGA-LIHC
high risk
low risk
Survival rate
p = 5.82e-05
Time (Years)
ROC curve (AUC = 0.649)
True positive rate
False positive rate
e
Points
Gender
Female
Male
Age
Stage
Stage I
Stage II
Stage III
Stage IV
Grade
G1
G2
G3
G4
riskScore
Total Points
1−year survival
3−year survival
5−year survival
C
a
Validation set
Risk score
Patients (increasing risk score)
b
Alive
Dead
Survival time (Years)
Patients (increasing risk score)
c
Risk score: Low
Risk score: High
KIF20A
KIF11
KIF2C
KIF4A
KIF14
KIF10
KIF18B
KIF23
d
eight-KIF gene in ICGC-LIRI-JP
high risk
low risk
Survival rate
p = 2.499e-07
Time (Years)
ROC curve (AUC = 0.775)
True positive rate
False positive rate
e
Points
Gender
Female
Male
Age
Stage
Stage I
Stage II
Stage III
Stage IV
priormalignancy
No
Yes
riskScore
Total Points
1−year survival
3−year survival
5−year survival

Figure 5. Eight KIF-gene prognostic signature biomarker performances in the training cohort and validation cohort. A. Prognostic gene analysis and signature generation pipeline. B, C. (a) The risk scores for all patients in the datasets are plotted in ascending order and marked as low risk (bottle green) or high risk (red), as distinguished by the threshold (vertical dashed line). (b) Survival status according to the eight prognostic genes in all patients of the two datasets. Dark red indicates deceased, and dark green indicates alive. (c) Heatmap of the eight prognostic genes in the training dataset or validation dataset with differential expression between the high- and low-risk groups. Dark red indicates higher expression, and light green indicates lower expression. (d, left) Kaplan-Meier estimates for the OS of patients stratified by the eight-KIF gene prognostic signature into high and low risk. (d, right) The ROC curve showing the false positive rate and true positive rate for the prediction of survival by the eight-KIF gene signature. (e) HCC survival nomogram, whereby an individual patient's value is located on each variable axis, and a line is drawn upward to determine the number of points received for each variable according to its value. The sum of these numbers is located on the Total Points axis, and a line is drawn downward to the survival axes to determine the likelihood of 1-, 3- and 5-year survival.

using the R package survival. Heatmaps were generated in TreeView with z-score normalization within each row (gene). Receiver operating characteristic (ROC) curves were then used to compare its prognostic validity with that of the eight-KIF gene signature risk model performed in the survival ROC package. We formulated nomograms using the rms package in R that included sex, age, clinical stage, pathological grading or prior malignancy. Statistical analyses were performed in R (version 3.5.0), and *p* values of less than 0.05 were deemed significant.

Cell lines and culture conditions

The HCC cell lines SK-Hep-1, Huh7, and HepG2 were purchased from the American Type Culture Collection (ATCC, USA). The HCC cell lines BEL-7404 and HCC-LM3 and the normal human liver epithelial cell line HL-7702 were purchased from the Institute of the Chinese Academy of Sciences (Shanghai, China). All cells were cultured in DMEM (HyClone, USA) supplemented with 10% fetal bovine serum (FBS, Gibco) at 37°C with 5% CO_2. The cell lines used in this study were not contaminated by mycoplasma.

Flow cytometry analysis

For DNA content analysis, cells were harvested and fixed in 75% methanol at -20°C overnight, rinsed twice with phosphate-buffered saline (PBS), rehydrated, resuspended in PBS containing 2 μg/mL propidium iodide (PI) and 5 μg/mL RNase A and analyzed using a BD FACSCalibur Flow Cytometer.

Colony formation assays

Five hundred cancer cells were seeded into cell culture plates, maintained in basal medium containing 10% FBS and allowed to grow for 7 days. The cells were then fixed with 4% paraformaldehyde (Solarbio, English) and stained with 0.5% crystal violet (Sigma Aldrich, St. Louis, MO, USA). The number of stained colonies was counted and analyzed.

Western blotting

Cells were harvested and washed with PBS and lysed in RIPA buffer containing a protease inhibitor cocktail (CWbio, China) and phosphatase inhibitor cocktail (CWbio, China) at 4°C for 30 min. The protein concentration was measured using a BCA protein assay kit (CWbio, China). Whole-cell extracts were boiled in SDS-PAGE loading buffer (Beyotime, China) at 100°C for 10 min. The proteins were separated by 10% SDS polyacrylamide gel electrophoresis and transferred to a 0.45 μm PVDF membrane (Merck Millipore, USA). The blots were incubated with 5% BSA to block nonspecific antigens and then with primary antibodies against KIF2C (Absci, USA, AB32855, 1:500 dilution), KIF4A (ABclonal, USA, A10193, 1:500 dilution), KIF10 (Proteintech, USA, 28142-1-AP, 1:500 dilution), KIF11 (Proteintech, USA, 23333-1-AP, 1:500 dilution), KIF14 (ABclonal, USA, A10275, 1:500 dilution), KIF18B (Abcam, USA, ab168-812, 1:500 dilution), KIF20A (Absci, USA, AB36573, 1:500 dilution), KIF23 (Affbiotech, US, DF2573, 1:500 dilution), CDK4 (Abcam, USA, ab108357, 1:1000 dilution), Phospho-Rb (Ser780) (D59B7) (Cell Signaling Technology, USA, 8180T, 1:1000 dilution), p53 (Cell Signaling Technology, USA, 9285T, 1:1000 dilution), and p21 (Proteintech, USA, 10355-1-AP, 1:500 dilution). After rinsing in TBST buffer three times for 10 min each, the blots were incubated with secondary antibodies at room temperature for 1 h. Immune complexes were detected using an ECL kit (Millipore Sigma,

USA). The amounts of protein relative to the loading control were quantified using ImageJ software.

RNA extraction and qRT-PCR

Total RNA was extracted from cultured cells using RNAiso Plus (TaKaRa, Dalian, China) following the manufacturer's instructions. Total RNA (1,000 ng) was reverse transcribed into cDNA using FastKing RT Kit (catalog KR116; Tiangen Biotech, Beijing, China). PCR analysis was performed using SYBR Green Talent qPCR PreMix (catalog FP209; Tiangen Biotech, Beijing, China) with a Bio-Rad CFX Connect Real-Time PCR System (Bio-Rad Laboratories, USA). The housekeeping gene GAPDH was used as a control. All primers (Table S11) used in this study were synthesized by Sangon Biotech (Shanghai, China).

Transfection

To silence KIF2C/4A/10/11/14/18B/20A/23, siRNAs (Table S12) that specifically target distinct KIF members were designed and synthesized. HCC cells were seeded into 6-well plates and transfected with siRNA or negative control (siRNA-NC) using Lipofectamine 3000 (Invitrogen, USA).

Cell proliferation analysis

Cell proliferation was measured by a Cell Counting Kit-8 (Dojindo Laboratories). HCC cells were seeded into 96-well plates and cultured in complete medium; cell viability was assessed every day for four days according to the manufacturer's instructions. Cell proliferation curves were plotted using the absorbance at each time point with GraphPad Prism 5.0 software. Statistics were calculated after three independent experiments were performed for each group.

Immunohistochemistry assays

Paraffin-embedded sections (4 μm) of tumor tissues or normal liver tissues were serially cut and used to detect kinesin superfamily members. Serial sections were baked at 65°C for 2 h and then deparaffinized and hydrated by sequentially washing in xylene, 100% ethanol, 95% ethanol, 85% ethanol, 75% ethanol and H_2O. The sections were boiled in citrate buffered saline + EDTA buffer (Leagene, Guangzhou, China) at 95°C for 15 min for antigen retrieval, and endogenous peroxidase (ZSbio, Beijing, China) was used to block the slides. After blocking nonspecific antigens with goat serum (BOSTER, Beijing, China), the slides were incubated with primary antibodies at 37°C for 1 h. The sections were washed with PBS three times for 3 min and incubated with a goat anti-rabbit horseradish peroxidase-conjugated antibody (ZSbio, Beijing, China) at room temperature for 20 min. The slides were then washed with PBS and developed with 3,3'-diaminobenzidine. The nuclei were stained with Gill's hematoxylin solution for 1 min, and the slides were then dehydrated, air-dried, and mounted. Images were captured using a Leica Microscope System (DM2500, CCD (DMC4500), Leica, Germany).

Statistical methods

OS and DFS were calculated using the Kaplan-Meier method and the log-rank test. Cox regression analysis was applied to evaluate the association of clinical parameters and KIF mRNA expression with HCC patient survival in R. Distributions between groups were compared by Student's t test for continuous variables and the χ^2 test for categorical variables. Distributions of the characteristics among three or more groups were compared by ANOVA. A P value < 0.05 was considered statistically significant. Significant p values are represented as *P ≤ 0.05, **P ≤ 0.01, and ***P < 0.001, and n.s. indicates no significance.

Results

Overexpression of different KIF family members in patients with HCC

To explore the potential prognosis and therapeutic value of different KIF members in HCC, we analyzed the mRNA and protein expression levels of KIF members using three public databases (www.oncomine.org (ONCOMINE); http://ualcan.path.uab.edu (UALCAN); http://www.proteinatlas.org/. (Human Protein Atlas)). As shown in **Figure 1A** and **Table 1**, among the 43 KIFs, mRNA expression of KIF2C/4A/10/11/14/18B/20A/23 was high in liver cancer tissues compared to normal tissues according to the ONCOMINE database. The de-

Table 1. Significant changes in KIF expression at the transcriptional level between HCC and normal liver tissues (ONCOMINE)

	Types of HCC VS. Liver	Fold change	*P* Value	T-test	Ref.
KIF2C	Hepatocellular Carcinoma	3.462	4.20E-7	5.958	Wurmbach Liver
	Hepatocellular Carcinoma	2.169	3.95E-48	17.795	Roessler Liver 2
	Hepatocellular Carcinoma	2.867	5.84E-7	6.561	Roessler Liver
KIF4A	Hepatocellular Carcinoma	4.704	1.88E-9	7.769	Wurmbach Liver
	Hepatocellular Carcinoma	2.704	3.54E-62	22.006	Roessler Liver 2
	Hepatocellular Carcinoma	2.665	4.05E-8	7.415	Roessler Liver
KIF10	Hepatocellular Carcinoma	3.123	4.48E-8	6.758	Wurmbach Liver
KIF11	Hepatocellular Carcinoma	3.846	1.84E-8	7.052	Wurmbach Liver
	Hepatocellular Carcinoma	2.690	4.05E-12	7.504	Chen Liver
KIF14	Hepatocellular Carcinoma	5.344	9.34E-14	10.605	Wurmbach Liver
	Hepatocellular Carcinoma	2.406	2.19E-8	7.893	Roessler Liver
KIF18B	Hepatocellular Carcinoma	2.093	3.22E-8	7.182	Roessler Liver
	Hepatocellular Carcinoma	2.680	6.23E-6	5.081	Wurmbach Liver
KIF20A	Hepatocellular Carcinoma	6.336	8.38E-11	8.766	Wurmbach Liver
	Hepatocellular Carcinoma	3.252	2.47E-68	24.329	Roessler Liver 2
	Hepatocellular Carcinoma	2.711	5.62E-8	7.398	Roessler Liver
KIF23	Hepatocellular Carcinoma	2.253	3.93E-17	9.286	Chen Liver
	Hepatocellular Carcinoma	2.143	2.17E-5	4.633	Wurmbach Liver

tailed expression patterns of these eight KIFs are listed in **Table 1**. Next, we further analyzed the mRNA expression patterns of these eight KIF members using UALCAN, which obtains data from The Cancer Genome Atlas (TCGA) projects; and analyzed the RNA sequencing data using a standard processing pipeline. As illustrated in **Figure 1B**, the mRNA expression levels of these eight distinct KIFs were significantly higher in HCC than in normal liver tissues.

We also explored the protein expression of these eight KIF superfamily members in the Human Protein Atlas. KIF18B was not detected in normal liver tissues and HCC. KIF4A, KIF14 and KIF20A exhibited weak intensity in normal tissues and moderate intensity in tumor tissues. KIF10 was negative in normal tissues and moderately positive in tumor tissues, and KIF11 and KIF23 showed the same expression intensity in normal tissues and tumor tissues (Figure S1). We then used immunohistochemical staining to detect the protein expression of these eight KIF members in the cancer tissues and normal liver tissues of 15 patients with liver cancer. As presented in **Figure 2**, KIF2C/KIF14 protein expression was upregulated in tumor tissues compared to normal tissues in 14 of 15 cases, KIF4A/KIF10/KIF11/KIF18B was upregulated in tumor tissues in 13 of 15 cases, and KIF-20A/KIF23 was highly expressed in tumor tissues compared to normal tissues in 12 of 15 cases.

In summary, the results indicate that the eight kinesin superfamily members are overexpressed at both the mRNA and protein levels of in patients with HCC.

Association of the mRNA expression of different KIF family members with the clinicopathological parameters of HCC patients

We then assessed the relationship between the mRNA expression of these eight KIF members and the clinicopathological parameters of HCC patients using UALCAN. As shown in **Figure 3A**, all eight KIFs were associated with the staging and grading of HCC patients. Although the mRNA levels of KIFs in stage III were higher than those in the normal group and stage I/II, there was no significant difference in the mRNA expression level of the eight KIFs between stage IV and other stages, likely because the number of samples in stage IV was small (n=6). The pathological grade of HCC is known to be directly related to patient prognosis. In our analysis, KIF11 and KIF14 mRNAs

Table 2. Correlation between KIF expression and clinicopathologic characteristics of HCC patients

Characteristics KIFs	*p* value							
	KIF2C	KIF4A	KIF10	KIF11	KIF14	KIF18B	KIF20A	KIF23
Age (Years)								
≤ 61	0.052	0.083	0.128	0.01*	0.052	0.003*	0.024*	0.001*
> 61								
Sex								
Male	0.075	0.119	0.075	0.119	0.119	0.026*	0.075	0.119
Female								
Cirrhosis								
Free	0.723	0.796	0.454	0.176	0.18	0.342	0.147	0.176
Established								
Adjacent hepatic tissues inflammation								
None	0.39	0.122	0.865	0.842	0.574	0.636	0.325	0.36
Mild								
Severe								
AFP, ug/L								
≤ 15	0.001*	0.001*	0.001*	0.001*	0.001*	0.001*	0.001*	0.001*
> 15								
Vascular invasion								
None	0.115	0.033*	0.048*	0.346	0.305	0.272	0.237	0.272
Micro								

AFP: α-fetoprotein; *represents statistically significant differences ($p < 0.05$).

were highest in grade 3 ($P < 0.05$); the mRNA levels of the other six KIF members increased with the tumor grade (**Figure 3B**). We next analyzed the correlation of the high expression rates of the eight KIF members in HCC with respect to other clinicopathological features, including age, sex, cirrhosis, adjacent hepatic tissue inflammation, α-fetoprotein (AFP), and vascular invasion, as detailed in **Table 2**. The results demonstrated that high mRNA expression of these eight KIFs had a significant correlation with the patient's AFP concentration; additionally, high KIF4A/KIF10 mRNA was related to microvascular invasion. The mRNA expression level of KIF11/KIF18B/KIF20A/KIF23 unexpectedly showed a correlation with age, and KIF18B exhibited a correlation with sex among patients with HCC (**Table 2**). Overall, the mRNA expression of these eight KIF members was significantly associated with the clinicopathological parameters of HCC patients.

High mRNA expression of KIF2C/4A/10/11/14/18B/20A/23 in HCC tissues correlates with poor patient survival

Furthermore, we used Gene Expression Profiling Interactive Analysis (GEPIA, http://gepia.cancer-pku.cn/index.html) to analyze the prognostic values of the eight KIF superfamily members in HCC. Interesting results were obtained: in particular, the high mRNA expression of the above eight KIFs was associated with poor overall survival (OS) and disease-free survival (DFS) prognoses of liver cancer patients ($P < 0.05$) (**Figure 4A**, **4B**). In addition, univariate analysis using the Cox proportional hazards model indicated tumor stage and high mRNA expression of all eight KIF family members were associated with poor survival prognosis (**Table 3**), and multivariate analysis including the mRNA level of individual KIF members, age, sex, and disease stage showed that high mRNA expression of the eight KIFs to be a factor for predicting poor survival (Tables S1, S2, S3, S4, S5, S6, S7, S8). These results indicate that the mRNA levels of KIF2C/4A/10/11/14/18B/20A/23 are related to clinical prognosis and might be independent prognostic markers in patients with HCC.

The KIF2C/4A/10/11/14/18B/20A/23 signature predicts survival in patients with HCC

According to the above analyses, mRNA expression levels of KIF2C, KIF4A, KIF10, KIF11, KIF14, KIF18B, KIF20A, and KIF23 are posi-

Table 3. Univariate analysis of overall survival with various prognostic parameters in patients with HCC

	Hazard Ratio	z	*P*
Sex	1.42968	1.15991	0.246086
Age	1.673732	1.904736	0.056814
Weight	0.766984	-1.00983	0.312576
Liver fibrosis ishak score category	0.850763	-0.85885	0.390424
Adjacent hepatic tissue inflammation extent type	1.313585	0.795316	0.42643
AFP At Procurement (ug/L)	1.021282	0.959624	0.337245
Vascular Invasion	1.59652	1.29833	0.194174
Tumor Stage	2.602234	4.558501	5.15E-06*
Neoplasm Histologic Grade	1.253297	0.881582	0.378003
KIF2C	1.30525	4.708563	2.49E-06*
KIF4A	1.232156	3.8707	0.000109*
KIF10	1.310007	4.361925	1.29E-05*
KIF11	1.309257	3.842049	0.000122*
KIF14	1.226721	3.36548	0.000764*
KIF18B	1.232979	3.851613	0.000117*
KIF20A	1.321848	4.495012	6.96E-06*
KIF23	1.230367	3.786422	0.000153*

*represents statistically significant differences ($p < 0.05$).

tively associated with the OS of patients with HCC. We then constructed a signature using these eight KIFs by using a risk score method with the regression coefficients from this model, and the median value was chosen as the threshold. All 366 samples from TCGA PanCancer Atlas were included in the analysis and served as the training set; a group of 233 samples downloaded from the International Cancer Genome Consortium (ICGC) database (https://dcc.icgc.org/, Liver Cancer-RIKEN, JP) was used as the validation set (**Figure 5A**). The risk score was calculated as follows: (0.000845 × mRNA level of KIF2C) - (0.00015 × mRNA level of KIF4A) + (0.000614 × mRNA level of KIF10) - (0.00139 × mRNA level of KIF11) - (0.00024 × mRNA level of KIF14) + (0.000813 × mRNA level of KIF-18B) + (0.001172 × mRNA level of KIF-20A) - (0.0.00017 × mRNA level of KIF23). Low-risk patients, as defined by the eight-KIF signature-based risk scores, had significantly better OS ($P < 0.001$ in the cohort TCGA-LIHC; **Figure 5Ba-d**). Furthermore, the eight-KIF gene signature-based risk score model effectively predicted OS in patients with HCC in the validation dataset (**Figure 5Ca-d**). In addition, multivariate Cox regression analyses revealed the eight-KIF gene signature and clinical stage to be independent prognostic predictors for OS (**Table 4**). The prognostic nomograms integrating sex, age, stage, risk score, grade (training set) or prior malignancy (validation set) for OS in the two cohorts are shown in **Figure 5Be**, **5Ce**.

Identification of the signaling pathways and oncogenic signatures correlated with the eight-gene signature

We further explored the functional implications of these identified prognostic genes in HCC tumorigenesis and development and performed bioinformatics analysis to predict gene functions. By determining the prognostic model via gene set enrichment analysis (GSEA) TCGA profiles, we obtained 32 pathways and 19 gene sets ($P < 0.01$). Kyoto Encyclopedia of Genes and Genomes (KEGG) enrichment analysis showed that the eight KIF genes are involved in multiple cancer-related pathways, such as the cell cycle, the p53 signaling pathway, the PPAR signaling pathway and DNA replication (**Figure 6A** and Table S9). The results of oncogenic signature enrichment analysis showed that the expression of these eight KIF members correlated positively with several oncogenes, such as CSR_LATE gene signatures (CSR_LATE_UP.V1_UP) and E2F1 gene signatures (E2F1_UP.V1_UP). High expression of KIFs correlated negatively with RB-activated gene signatures

Table 4. Univariate and multivariate Cox regression analyses of survival according to the eight-KIF signature in the training set and the validation set of HCC patients

Training set (TCGA-LIHC)						
Variable	Univariate analysis			Multivariate analysis		
	HR	95% CI	*p*-Value	HR	95% CI	*p*-Value
Gender	1.3117	0.901-1.910	0.1567	1.1561	0.781-1.711	0.4685
Age	1.0129	0.998-1.028	0.0872	1.0126	0.997-1.028	0.1033
Stage	1.6557	1.354-2.024	0.0000	1.5891	1.288-1.960	0.0000
Grade	1.1398	0.888-1.464	0.3051	1.1567	0.884-1.514	0.2890
Risk score	1.2368	1.146-1.335	0.0000	1.1805	1.086-1.283	0.0001
Validation set (ICGA-LIRI-JP)						
Variable	Univariate analysis			Multivariate analysis		
	HR	95% CI	*p*-Value	HR	95% CI	*p*-Value
Gender	1.9286	1.037-3.594	0.0387	2.7536	1.450-5.228	0.002
Age	1.0020	0.972-1.033	0.8985	0.9937	0.961-1.028	0.7126
Stage	2.1546	1.493-3.110	0.0000	2.3469	1.626-3.387	0.0000
Grade	1.7510	0.773-3.965	0.1791	1.9613	0.802-4.798	0.1400
Risk score	2.58E+52	1.2E+35-5.2E+69	0.0000	7.37E+52	2.9E+34-1.9E+71	0.0000

HR: hazard ratio; CI: confidence interval.

(RB_P107_DN.V1_UP and RB_DN.V1_UP) (**Figure 6B** and Table S10).

KIF2C/4A/10/11/14/18B/20A/23 promote cell proliferation via regulating the G1-to-S transition of the cell cycle

As our pathway enrichment analysis suggested that the eight KIF superfamily members are enriched in the cell cycle in HCC, we further investigated the biological function of KIF2C/4A/10/11/14/18B/20A/23 in HCC cells in vitro. We first explored the expression levels of the eight KIFs in HCC cell lines and found increases in HCC cell lines compared with that in the normal human liver epithelial cell line HL-7702 (**Figure 7A**). Of the 5 HCC cell lines, we chose Huh7 cells, which showed a higher level of KIF mRNA, and HCC-LM3 cells, which exhibited a relatively lower level of KIF mRNA, to perform a loss-of-function experiment. We first designed siRNAs that specifically target distinct KIFs (**Figure 7B**). Interestingly, the CCK-8 and colony formation assays indicated that transient downregulation of distinct KIFs inhibited proliferation in both Huh7 and LM3 cells (**Figure 7C**). Considering that the eight KIF superfamily members might affect cell proliferation by regulating the cell cycle, we next explored HCC cell cycle arrest after downregulating the 8 KIFs by flow cytometry. As expected, loss of KIF2C/4A/10/11/14/18B/20A/23 resulted in increased G1 arrest and p53 and p21 expression and decreased CDK4 and phospho-Rb expression in HCC cells (**Figure 8**). These results indicated that silencing the eight KIF superfamily members KIF2C/4A/10/11/14/18B/20A/23 efficiently prevent cell growth by inhibiting the cell cycle G1-to-S transition of HCC in vitro.

Discussion

Using public database analysis, we identified 8 of 45 kinesin superfamily members to be highly expressed in HCC tissues compared to normal liver tissues. Further analysis revealed that eight KIFs (KIF2C, KIF4A, KIF10, KIF11, KIF14, KIF18B, KIF20A, and KIF23) correlate positively with clinical parameters, including tumor stage, tumor grade, and serum AFP concentration. Furthermore, high expression of these eight KIFs correlated with worse survival in HCC patients. A risk score index using these eight KIFs effectively predicted the OS rate of patients with HCC. Consistent with the GSEA analysis result that the 8 KIFs are involved in the cell cycle in HCC cells, our in vitro experiment showed that reducing expression of these KIFs efficiently inhibited cell growth by promoting G1-phase arrest. These results suggest that KIFs play important roles in the development and progression of HCC

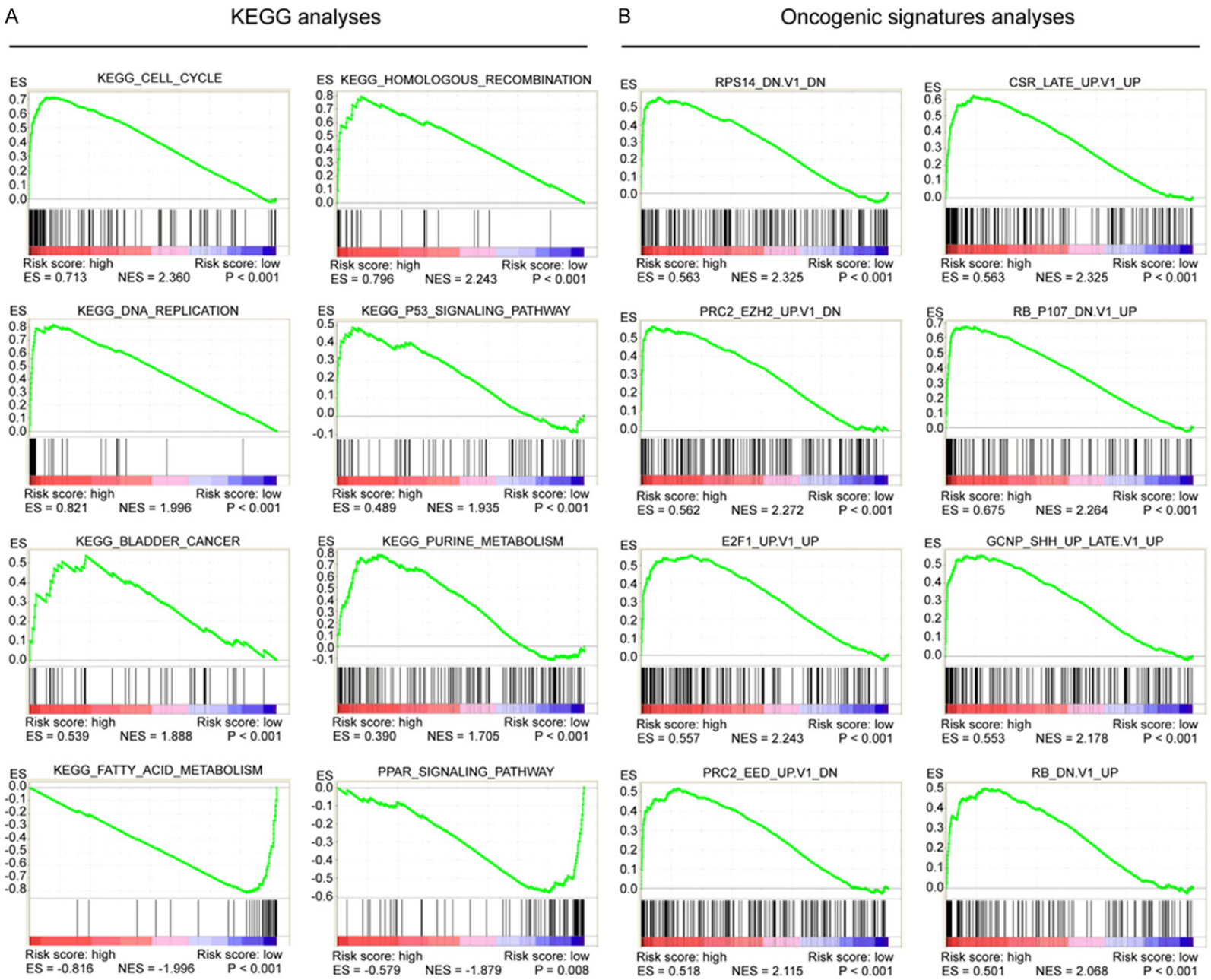
A
KEGG analyses
B
Oncogenic signatures analyses
KEGG_CELL_CYCLE
Risk score: high
Risk score: low
ES = 0.713 NES = 2.360 P < 0.001
KEGG_HOMOLOGOUS_RECOMBINATION
ES = 0.796 NES = 2.243 P < 0.001
RPS14_DN.V1_DN
ES = 0.563 NES = 2.325 P < 0.001
CSR_LATE_UP.V1_UP
ES = 0.563 NES = 2.325 P < 0.001
KEGG_DNA_REPLICATION
ES = 0.821 NES = 1.996 P < 0.001
KEGG_P53_SIGNALING_PATHWAY
ES = 0.489 NES = 1.935 P < 0.001
PRC2_EZH2_UP.V1_DN
ES = 0.562 NES = 2.272 P < 0.001
RB_P107_DN.V1_UP
ES = 0.675 NES = 2.264 P < 0.001
KEGG_BLADDER_CANCER
ES = 0.539 NES = 1.888 P < 0.001
KEGG_PURINE_METABOLISM
ES = 0.390 NES = 1.705 P < 0.001
E2F1_UP.V1_UP
ES = 0.557 NES = 2.243 P < 0.001
GCNP_SHH_UP_LATE.V1_UP
ES = 0.553 NES = 2.178 P < 0.001
KEGG_FATTY_ACID_METABOLISM
ES = -0.816 NES = -1.996 P < 0.001
PPAR_SIGNALING_PATHWAY
ES = -0.579 NES = -1.879 P = 0.008
PRC2_EED_UP.V1_DN
ES = 0.518 NES = 2.115 P < 0.001
RB_DN.V1_UP
ES = 0.501 NES = 2.068 P < 0.001

Figure 6. Identification of the signaling pathways and oncogenic signatures correlating with the eight-gene signature. A. KEGG analyses of the pathways of prognosis-related genes. B. GSEA plot showing that the prognosis-related genes correlate with multiple gene signatures.

and might serve as prognostic biomarkers and potential therapeutic targets in HCC.

Blocking mitotic exit is believed to be a promising anticancer strategy to overcome chemotherapy resistance [25, 26]. KIFs have been shown to play important roles in MT-dependent intracellular transport and are crucial for mitosis, emerging as targets for chemotherapeutic intervention [5]. Although several compounds targeting mitotic kinesins are effective in animal models, the same efficacy does not appear to translate to human treatment, limiting its widespread use in clinical practice. Nonetheless, when combined with other drugs, some compounds increase the sensitivity of chemotherapy drugs in certain cancers, such as breast cancer [11], indicating the potential clinical value of compounds that specifically target KIFs.

KIF2C (also known as MCAK) depolymerizes MTs, regulating the location of lysosomes in the cytoplasm [27]. KIF2C has been found to be upregulated in colorectal cancer, breast cancer and gastric cancer tissues compared with corresponding nonmalignant tissues and is significantly associated with lymphatic invasion, lymph node metastasis and OS of patients with cancer [27-29]. KIF2C is precisely controlled in time and space by multiple molecules such as Sgo2 and Aurora A/B [30, 31]. Clinical data show that silencing MCAK or interfering with its regulatory protein significantly reduces the invasion rate of carcinoma cells [32]. In our study, KIF2C mRNA and protein were highly expressed in HCC tissues compared to normal tissues, and KIF2C was significantly associated with tumor stage, tumor grade and serum AFP concentration, in accordance with the findings of previous studies [27]. Moreover, higher expression of KIF2C was significantly related to poorer OS in HCC patients and served as an independent prognostic factor for shorter OS in patients with HCC, indicating that KIF2C participates in the tumorigenesis of HCC.

The gene expressing kinesin family member 4A (KIF4A) is located at Xq13.1 in the human genome, and the 140-kDa protein is mainly located in the nucleus [33]. KIF4A is remarkably upregulated in primary cancers such as colorectal cancer and breast cancer, and elevated expression of KIF4A in cancer tissues correlated significantly with patient clinicopathological characteristics and shorter overall and disease-free cumulative survival in cancer [34-36]. In addition, expression of KIF4A in non-small cell lung cancer cells significantly affects cisplatin resistance [37]. Based on those studies, KIF4A might be a chemotherapy resistance-associated protein and serve as a potential target for chemotherapeutic drug resistance in cancers. We observed significantly higher mRNA and protein expression of KIF4A in HCC tissues, and the mRNA expression of KIF4A correlated markedly with individual cancer stages and tumor grades. In addition, a higher mRNA expression of KIF2C was significantly related to poorer OS in liver cancer patients, serving as an independent prognostic factor for shorter OS and indicating that KIF4A plays an oncogenic role in HCC.

Centromere protein E (CENPE, also known as KIF10) is a human kinetochore protein that is highly expressed in the G2/M phase of the cell cycle. Previous studies have revealed that CENPE is highly expressed in lung adenocarcinoma tissues and prostate cancer and is involved in the development of cancers [38, 39]. KIF10 is tightly controlled by transcription factors such as FOXM1. Knockdown of KIF10 or interference with these transcription factors results in decreased lung cancer cell proliferation [38]. In our present study, KIF10 was found to be upregulated in liver cancer tissues compared with normal liver tissues, correlating with the clinicopathological features of patients with HCC. As KIF10 knockdown by siRNAs inhibited cell proliferation and promoted G1 phase arrest, KIF10 is a novel potential therapeutic target in HCC.

Eg5, also known as kinesin-5, KIF11 or kinesin spindle protein, is responsible for centrosome separation in cell division [40]. KIF11 appears to be involved in the progression of glioblastoma. Silencing KIF11 with a specific small-molecule inhibitor blocked the growth of the more

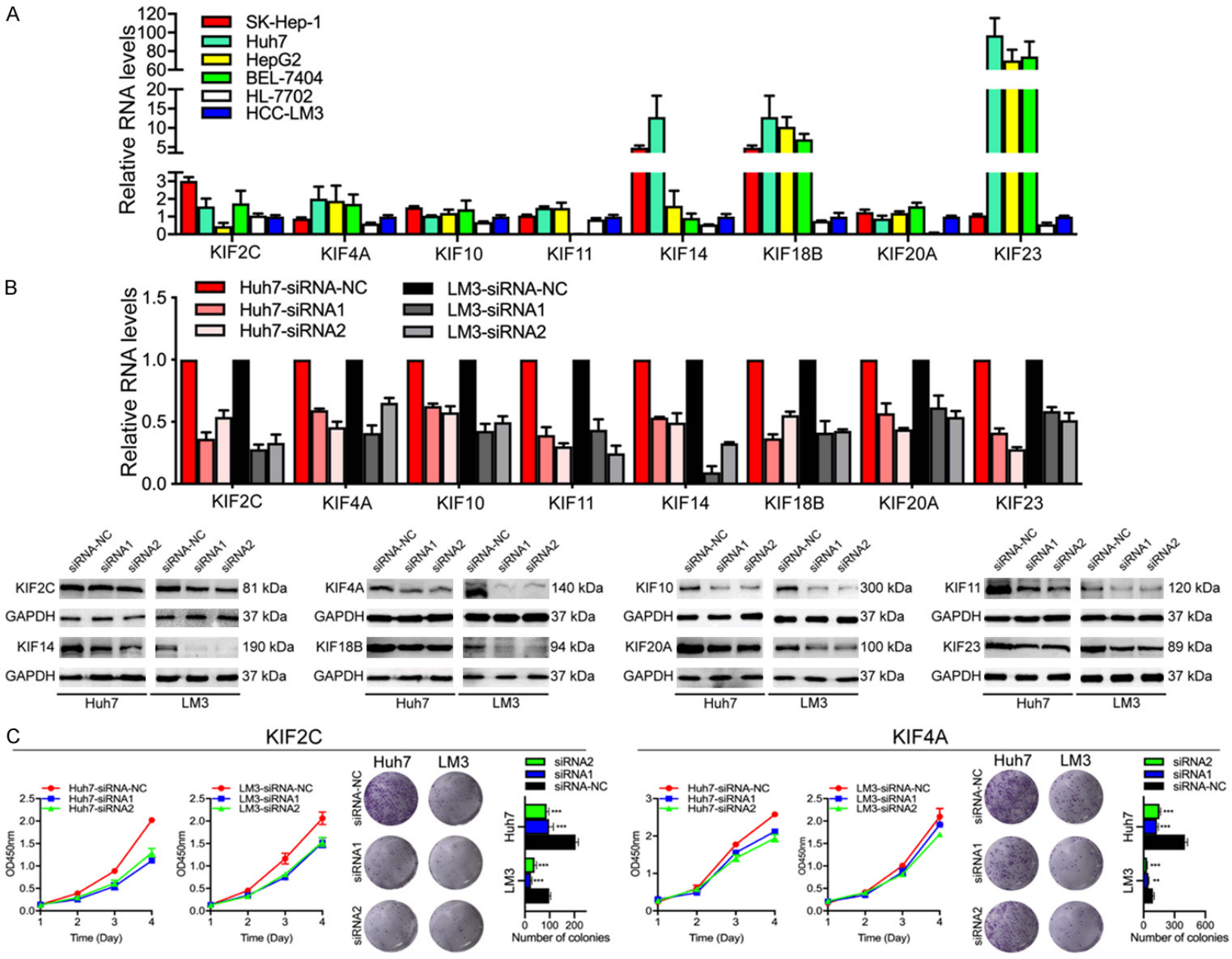
A
Relative RNA levels
SK-Hep-1
Huh7
HepG2
BEL-7404
HL-7702
HCC-LM3
KIF2C
KIF4A
KIF10
KIF11
KIF14
KIF18B
KIF20A
KIF23
B
Relative RNA levels
Huh7-siRNA-NC
Huh7-siRNA1
Huh7-siRNA2
LM3-siRNA-NC
LM3-siRNA1
LM3-siRNA2
siRNA-NC
siRNA1
siRNA2
KIF2C 81 kDa
GAPDH 37 kDa
KIF14 190 kDa
KIF4A 140 kDa
KIF18B 94 kDa
KIF10 300 kDa
KIF20A 100 kDa
KIF11 120 kDa
KIF23 89 kDa
Huh7
LM3
C
KIF2C
KIF4A
OD450nm
Time (Day)
Number of colonies

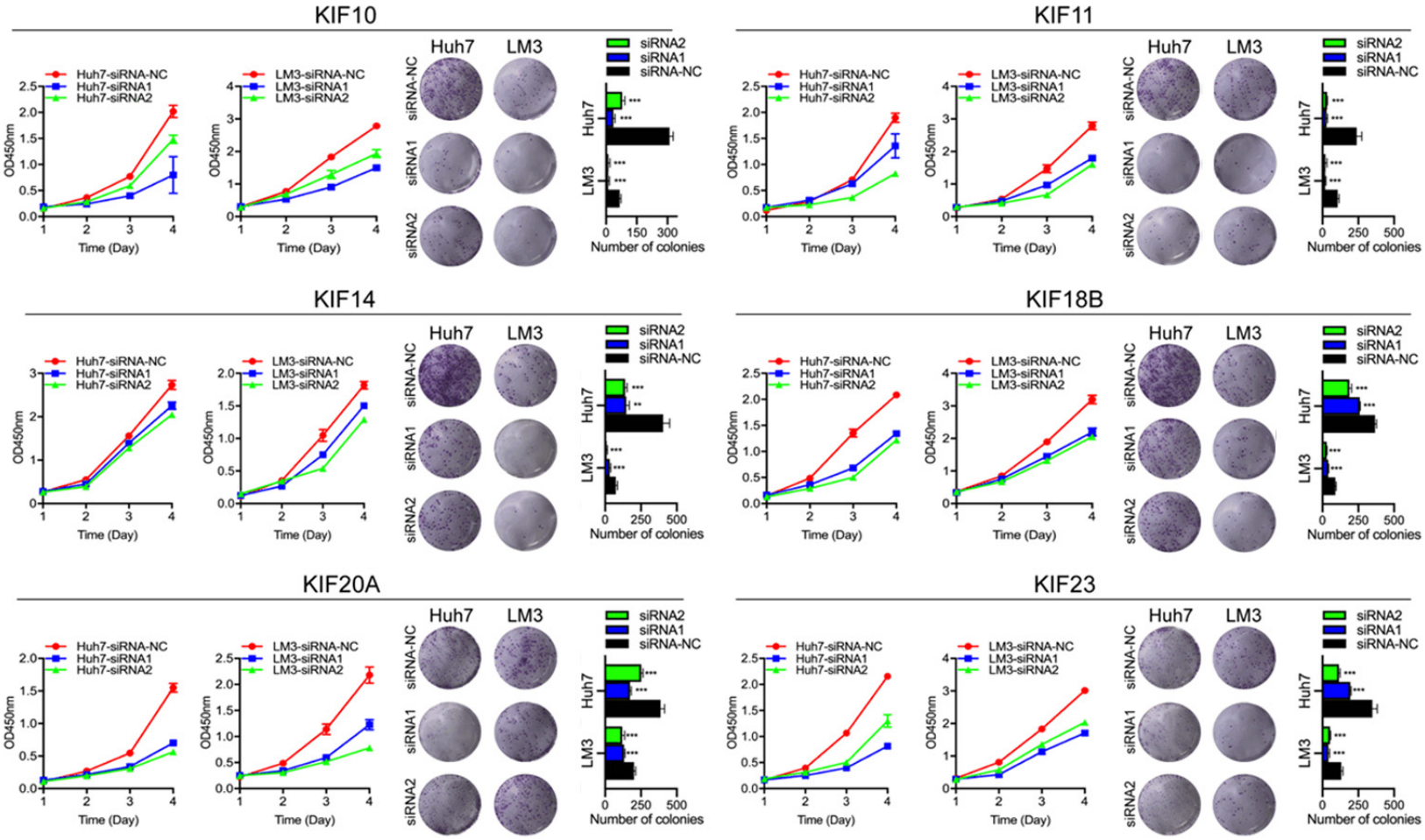

Figure 7. KIF2C/4A/10/11/14/18B/20A/23 promote cell proliferation in HCC. A. Eight KIFs were evaluated in liver cancer cell lines compared with the normal liver epithelial cell line HL-7702, as analyzed by qRT-PCR. B. Eight distinct KIFs were effectively knocked down by siRNAs. C. Knockdown of the eight KIFs inhibited HCC cell growth, as determined by the CCK-8 and colony formation assays. One-way ANOVA was used for statistical analysis.

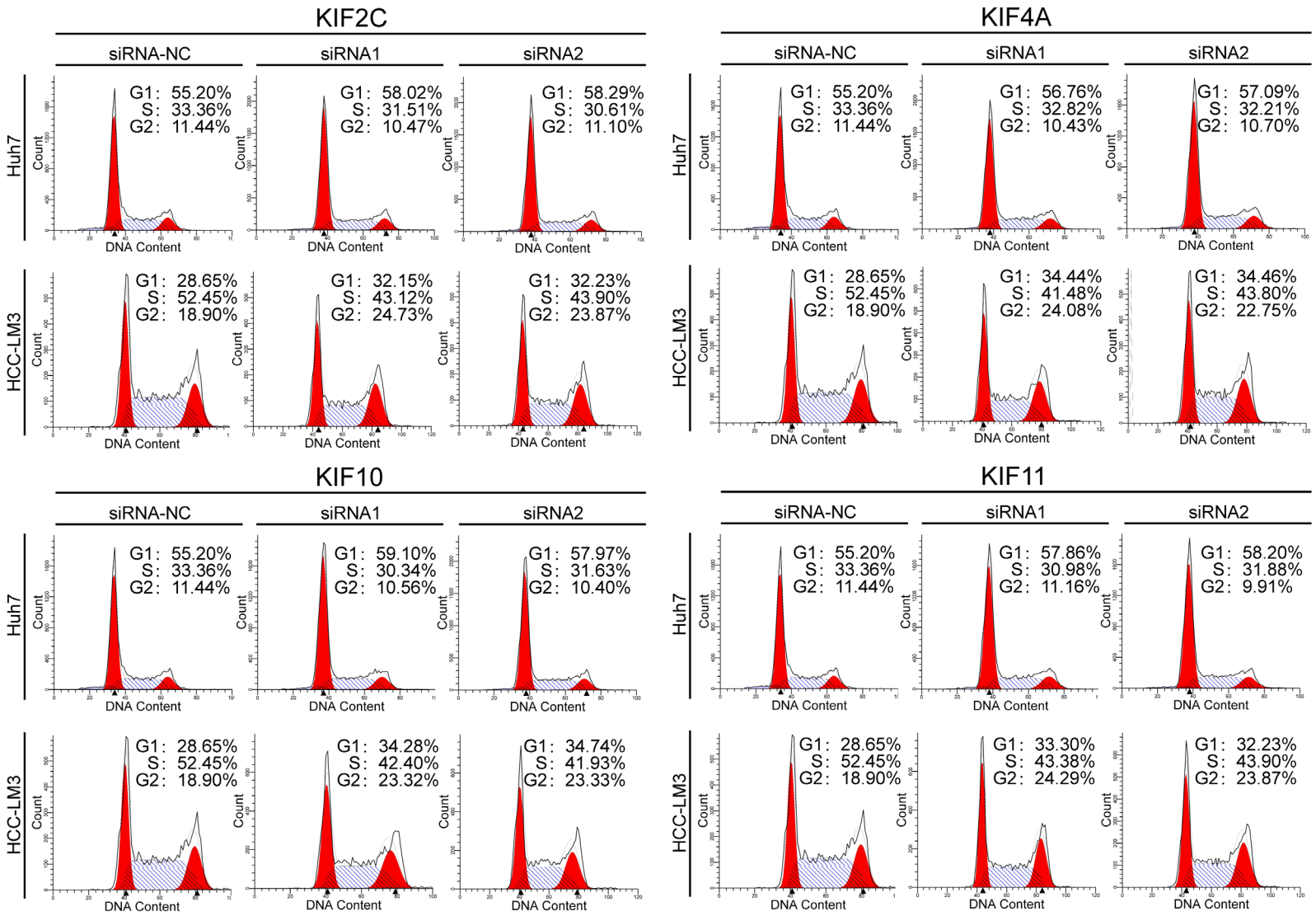
KIF2C
siRNA-NC
siRNA1
siRNA2
Huh7
G1: 55.20%
S: 33.36%
G2: 11.44%
G1: 58.02%
S: 31.51%
G2: 10.47%
G1: 58.29%
S: 30.61%
G2: 11.10%
HCC-LM3
G1: 28.65%
S: 52.45%
G2: 18.90%
G1: 32.15%
S: 43.12%
G2: 24.73%
G1: 32.23%
S: 43.90%
G2: 23.87%
KIF4A
siRNA-NC
siRNA1
siRNA2
Huh7
G1: 55.20%
S: 33.36%
G2: 11.44%
G1: 56.76%
S: 32.82%
G2: 10.43%
G1: 57.09%
S: 32.21%
G2: 10.70%
HCC-LM3
G1: 28.65%
S: 52.45%
G2: 18.90%
G1: 34.44%
S: 41.48%
G2: 24.08%
G1: 34.46%
S: 43.80%
G2: 22.75%
KIF10
siRNA-NC
siRNA1
siRNA2
Huh7
G1: 55.20%
S: 33.36%
G2: 11.44%
G1: 59.10%
S: 30.34%
G2: 10.56%
G1: 57.97%
S: 31.63%
G2: 10.40%
HCC-LM3
G1: 28.65%
S: 52.45%
G2: 18.90%
G1: 34.28%
S: 42.40%
G2: 23.32%
G1: 34.74%
S: 41.93%
G2: 23.33%
KIF11
siRNA-NC
siRNA1
siRNA2
Huh7
G1: 55.20%
S: 33.36%
G2: 11.44%
G1: 57.86%
S: 30.98%
G2: 11.16%
G1: 58.20%
S: 31.88%
G2: 9.91%
HCC-LM3
G1: 28.65%
S: 52.45%
G2: 18.90%
G1: 33.30%
S: 43.38%
G2: 24.29%
G1: 32.23%
S: 43.90%
G2: 23.87%
Count
DNA Content

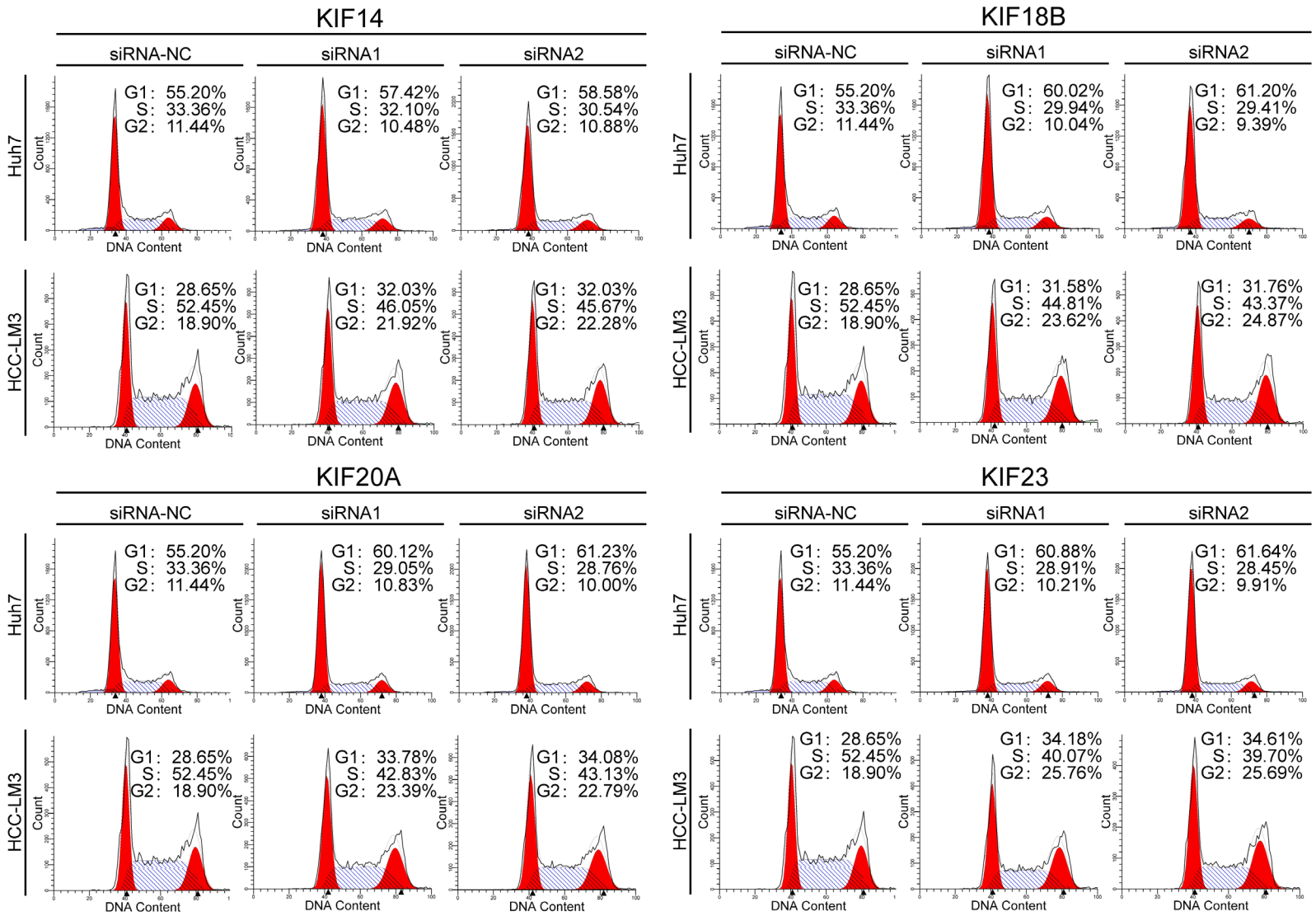
KIF14
siRNA-NC
siRNA1
siRNA2
Huh7
G1: 55.20%
S: 33.36%
G2: 11.44%
G1: 57.42%
S: 32.10%
G2: 10.48%
G1: 58.58%
S: 30.54%
G2: 10.88%
HCC-LM3
G1: 28.65%
S: 52.45%
G2: 18.90%
G1: 32.03%
S: 46.05%
G2: 21.92%
G1: 32.03%
S: 45.67%
G2: 22.28%
KIF18B
siRNA-NC
siRNA1
siRNA2
Huh7
G1: 55.20%
S: 33.36%
G2: 11.44%
G1: 60.02%
S: 29.94%
G2: 10.04%
G1: 61.20%
S: 29.41%
G2: 9.39%
HCC-LM3
G1: 28.65%
S: 52.45%
G2: 18.90%
G1: 31.58%
S: 44.81%
G2: 23.62%
G1: 31.76%
S: 43.37%
G2: 24.87%
KIF20A
siRNA-NC
siRNA1
siRNA2
Huh7
G1: 55.20%
S: 33.36%
G2: 11.44%
G1: 60.12%
S: 29.05%
G2: 10.83%
G1: 61.23%
S: 28.76%
G2: 10.00%
HCC-LM3
G1: 28.65%
S: 52.45%
G2: 18.90%
G1: 33.78%
S: 42.83%
G2: 23.39%
G1: 34.08%
S: 43.13%
G2: 22.79%
KIF23
siRNA-NC
siRNA1
siRNA2
Huh7
G1: 55.20%
S: 33.36%
G2: 11.44%
G1: 60.88%
S: 28.91%
G2: 10.21%
G1: 61.64%
S: 28.45%
G2: 9.91%
HCC-LM3
G1: 28.65%
S: 52.45%
G2: 18.90%
G1: 34.18%
S: 40.07%
G2: 25.76%
G1: 34.61%
S: 39.70%
G2: 25.69%
Count
DNA Content

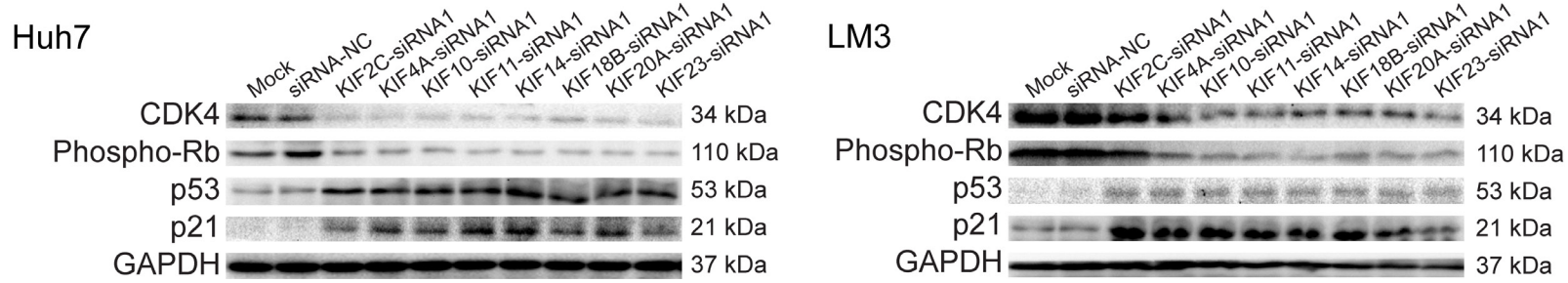

Figure 8. Knocking down eight different KIF members increased G1-phase arrest in HCC cells, as demonstrated by flow cytometry and western blotting.

treatment-resistant glioblastoma tumor-initiating cells (TICs) as well as non-TICs and hindered tumor initiation and self-renewal of the TIC population. Moreover, targeting KIF11 reduced glioma cell invasion in an animal model [41]. Inhibitors of KIF11 have entered clinical trials for monotherapy or in combination with other drugs for tumor treatment [42]. Here, we show that a high expression of KIF11 in tumor tissues correlates positively with worse OS in patients with HCC, and KIF11 was found to be an independent prognostic factor for shorter OS in liver cancer patients. Furthermore, knockdown of KIF11 significantly delayed cell growth and promoted G1-phase arrest in HCC. Our data indicate that KIF11 might be involved in the progression of HCC as in other cancers.

KIF14 also plays multiple roles in the progression of various solid tumors, including breast cancer, lung cancer, retinoblastoma, laryngeal cancer, pancreatic cancer, and ovarian carcinoma [43-48]. Overexpression of KIF14 significantly decreases the OS and DFS of cancer patients, suggesting that KIF14 is an independent prognostic factor in cancers [43, 46, 47]. In addition, KIF14 knockdown decreases tumorigenicity in vitro; thus, it is a clinically relevant oncogene and a promising therapeutic target [47]. Based on multiple databases, we found that the mRNA level of KIF14 was higher in HCC tissues than in normal liver tissues. Downregulation of KIF14 by siRNAs reduced proliferation and promoted cell cycle arrest in HCC cells. Our results indicate the important role of KIF14 in HCC and that targeting KIF14 is a possible strategy to overcome tumor development.

In Yaqin Wu's study, KIF18B was found to function as a novel oncogene that promotes the tumorigenicity of cervical cancer cells by activating the Wnt/β-catenin signaling pathway [49]. KIF18 is also reported to be overexpressed in breast, lung, ovarian, liver, and renal cancer compared with that in normal tissue, acting as a prognostic factor for patients with cancer [50], and overexpression of KIF18B increases the proliferation of HCC and cervical cancer cells [49, 50]. In our study, mRNA and protein levels of KIF18B were increased in liver cancer tissues compared with that in normal liver tissues, and high KIF18B expression predicted poor prognosis in patients with HCC. Consistent with previous studies reporting that silencing KIF18B resulted in increased G1 phase arrest in Huh7 cells [50], we confirmed that knockdown of KIF18B promoted G1 arrest in LM3 cells. However, further verification is needed to determine whether interfering with KIF18B inhibits the progression of HCC in vivo.

A prognostic signature consisting of CENPA, KIF20A, PLK1, and NCAPG efficiently predicted the OS rate of HCC patients [51], suggesting that KIF20A is a potential biomarker in HCC. Additionally, silencing KIF20B increased cell cycle arrest in G1 phase and apoptosis in cancer cells and inhibited tumor invasion and metastasis [52-54]. Moreover, a mechanistic study showed that KIF20A is tightly regulated by E2F1 and that depletion of E2F1 or KIF20A leads to the deformation of MT structures, impairing cell motility and suppressing tumor metastasis [55]. Similarly, in our study, KIF20A was found to be highly expressed in HCC tissues compared to normal tissues, and mRNA expression of KIF20A was significantly related to patients' individual tumor stages and grades. KIF20A also correlated significantly with a shorter OS in liver cancer patients and was an independent prognostic factor for a poor prognosis. Our data demonstrate that KIF20A contributes to the development and progression of HCC and that KIF20A might be a novel prognostic biomarker in HCC treatment.

Increased expression of KIF23 has been found in lung cancer, malignant pleural mesothelioma, and gastric cancer and is associated with poor prognosis [56-58]. Additionally, a functional study showed that the knockdown of KIF23 resulted in a marked inhibition of gastric cancer cell proliferation in mice [58]. In the present study, significantly higher mRNA and protein expression of KIF23 was found in HCC tissues, and KIF23 mRNA expression was markedly related to individual cancer stages and tumor grades. Accordingly, higher mRNA expression of KIF23 correlated with shorter OS in HCC patients and was an independent prognostic factor for liver cancer patients. In summary, our results suggest that KIF23 plays an oncogenic role in HCC.

GSEA showed that KIF2C, KIF4A, KIF10, KIF11, KIF18B, KIF20A, and KIF23 are significantly

associated with the cell cycle, p53, RB and DNA replication, which are associated with their biological functions. Our functional experiments in two HCC cell lines confirmed their involvement in the regulation of proliferation and the cell cycle in vitro. The results require additional animal experimental validation.

There are some limitations in the present study. First, the information used in this study from open-access databases, and the medical parameters were not complete. Further studies that detect the protein expression of KIF genes in larger sample sizes are needed to validate our findings and to explore the clinical application of KIFs in the diagnosis and treatment of HCC. Second, because of the incomplete patient clinical information in the public datasets, we were unable to construct a comprehensive hazard score model depending on the expression level of KIFs for visual prediction. Finally, we did not explore the mechanisms of the distinct KIFs in HCC. We also did not verify the effects of silencing distinct KIFs on the tumor growth of HCC cells in animal models. Future studies should investigate the detailed functions of distinct KIFs in HCC.

Conclusion

We identified a novel KIF mRNA signature significantly associated with patient survival in HCC. This KIF signature can add prognostic value to the tumor staging and grading system, which may help facilitate more personalized therapy. Multicenter, large-scale, prospective studies and further mechanistic investigations are necessary to validate our findings before this signature can be used in the clinic.

Acknowledgements

This work was supported by the National Natural Science Foundation of China (Grant Numbers 81672267 and 81772457).

Disclosure of conflict of interest

None.

Address correspondence to: Jian Zhang, Department of Oncology, Zhujiang Hospital, Southern Medical University, 253 Industrial Avenue, Guangzhou, China. Tel: +86-13925091863; Fax: +86-020-61643888; E-mail: blacktiger@139.com; Guodong Chen, Department of Interventional Radiology, Guangzhou First People's Hospital, The Second Affiliated Hospital of South China University of Technology, No. 1 Panfu Road, Guangzhou, China. Tel: +86-13710631118; Fax: +86-020-81045945; E-mail: chen-guodong71@hotmail.com

References

[1] Bray F, Ferlay J, Soerjomataram I, Siegel RL, Torre LA and Jemal A. Global cancer statistics 2018: GLOBOCAN estimates of incidence and mortality worldwide for 36 cancers in 185 countries. CA Cancer J Clin 2018; 68: 394-424.

[2] Kanwal F and Singal AG. Surveillance for hepatocellular carcinoma: current best practice and future direction. Gastroenterology 2019; 157: 54-64.

[3] Lens SM, Voest EE and Medema RH. Shared and separate functions of polo-like kinases and aurora kinases in cancer. Nat Rev Cancer 2010; 10: 825-841.

[4] Dominguez-Brauer C, Thu KL, Mason JM, Blaser H, Bray MR and Mak TW. Targeting mitosis in cancer: emerging strategies. Mol Cell 2015; 60: 524-536.

[5] Rath O and Kozielski F. Kinesins and cancer. Nat Rev Cancer 2012; 12: 527-539.

[6] Miki H, Setou M, Kaneshiro K and Hirokawa N. All kinesin superfamily protein, KIF, genes in mouse and human. Proc Natl Acad Sci U S A 2001; 98: 7004-7011.

[7] Hirokawa N, Noda Y and Okada Y. Kinesin and dynein superfamily proteins in organelle transport and cell division. Curr Opin Cell Biol 1998; 10: 60-73.

[8] Rogers GC, Scholey JM and Sharp DJ. Microtubule motors in mitosis. Nature 2000; 407: 41-47.

[9] Vale RD and Fletterick RJ. The design plan of kinesin motors. Annu Rev Cell Dev Biol 1997; 13: 745-777.

[10] Diefenbach RJ, Mackay JP, Armati PJ and Cunningham AL. The C-terminal region of the stalk domain of ubiquitous human kinesin heavy chain contains the binding site for kinesin light chain. Biochemistry 1998; 37: 16663-16670.

[11] Lucanus AJ and Yip GW. Kinesin superfamily: roles in breast cancer, patient prognosis and therapeutics. Oncogene 2018; 37: 833-838.

[12] De S, Cipriano R, Jackson MW and Stark GR. Overexpression of kinesins mediates docetaxel resistance in breast cancer cells. Cancer Res 2009; 69: 8035-8042.

[13] Chung V, Heath EI, Schelman WR, Johnson BM, Kirby LC, Lynch KM, Botbyl JD, Lampkin

TA and Holen KD. First-time-in-human study of GSK923295, a novel antimitotic inhibitor of centromere-associated protein E (CENP-E), in patients with refractory cancer. Cancer Chemother Pharmacol 2012; 69: 733-741.

[14] Kantarjian HM, Padmanabhan S, Stock W, Tallman MS, Curt GA, Li J, Osmukhina A, Wu K, Huszar D, Borthukar G, Faderl S, Garcia-Manero G, Kadia T, Sankhala K, Odenike O, Altman JK and Minden M. Phase I/II multicenter study to assess the safety, tolerability, pharmacokinetics and pharmacodynamics of AZD4877 in patients with refractory acute myeloid leukemia. Invest New Drugs 2012; 30: 1107-1115.

[15] Liu X, Li Y, Zhang X, Liu X, Peng A, Chen Y, Meng L, Chen H, Zhang Y, Miao X, Zheng L and Huang K. Inhibition of kinesin family member 20B sensitizes hepatocellular carcinoma cell to microtubule-targeting agents by blocking cytokinesis. Cancer Sci 2018; 109: 3450-3460.

[16] Liu X, Zhou Y, Liu X, Peng A, Gong H, Huang L, Ji K, Petersen RB, Zheng L and Huang K. MPHOSPH1: a potential therapeutic target for hepatocellular carcinoma. Cancer Res 2014; 74: 6623-6634.

[17] Knox JJ, Gill S, Synold TW, Biagi JJ, Major P, Feld R, Cripps C, Wainman N, Eisenhauer E and Seymour L. A phase II and pharmacokinetic study of SB-715992, in patients with metastatic hepatocellular carcinoma: a study of the national cancer institute of Canada clinical trials group (NCIC CTG IND.168). Invest New Drugs 2008; 26: 265-272.

[18] Tang PA, Siu LL, Chen EX, Hotte SJ, Chia S, Schwarz JK, Pond GR, Johnson C, Colevas AD, Synold TW, Vasist LS and Winquist E. Phase II study of ispinesib in recurrent or metastatic squamous cell carcinoma of the head and neck. Invest New Drugs 2008; 26: 257-264.

[19] Lee CW, Belanger K, Rao SC, Petrella TM, Tozer RG, Wood L, Savage KJ, Eisenhauer EA, Synold TW, Wainman N and Seymour L. A phase II study of ispinesib (SB-715992) in patients with metastatic or recurrent malignant melanoma: a national cancer institute of Canada clinical trials group trial. Invest New Drugs 2008; 26: 249-255.

[20] Rhodes DR, Yu J, Shanker K, Deshpande N, Varambally R, Ghosh D, Barrette T, Pander A and Chinnaiyan AM. ONCOMINE: a cancer microarray database and integrated data-mining platform. Neoplasia 2004; 6: 1-6.

[21] Chandrashekar DS, Bashel B, Balasubramanya SAH, Creighton CJ, Ponce-Rodriguez I, Chakravarthi BVSK and Varambally S. UALCAN: a portal for facilitating tumor subgroup gene expression and survival analyses. Neoplasia 2017; 19: 649-658.

[22] Tomczak K, Czerwinska P and Wiznerowicz M. The Cancer Genome Atlas (TCGA): an immeasurable source of knowledge. Contemp Oncol (Pozn) 2015; 19: A68-77.

[23] Gao J, Aksoy BA, Dogrusoz U, Dresdner G, Gross B, Sumer SO, Sun Y, Jacobsen A, Sinha R, Larsson E, Cerami E, Sander C and Schultz N. Integrative analysis of complex cancer genomics and clinical profiles using the cBioPortal. Sci Signal 2013; 6: pl1.

[24] Subramanian A, Tamayo P, Mootha VK, Mukherjee S, Ebert BL, Gillette MA, Paulovich A, Pomeroy SL, Golub TR, Lander ES and Mesirov JP. Gene set enrichment analysis: a knowledge-based approach for interpreting genome-wide expression profiles. Proc Natl Acad Sci U S A 2005; 102: 15545-15550.

[25] Liu X, Chen Y, Li Y, Petersen RB and Huang K. Targeting mitosis exit: a brake for cancer cell proliferation. Biochim Biophys Acta Rev Cancer 2019; 1871: 179-191.

[26] Huang HC, Shi J, Orth JD and Mitchison TJ. Evidence that mitotic exit is a better cancer therapeutic target than spindle assembly. Cancer Cell 2009; 16: 347-358.

[27] Nakamura Y, Tanaka F, Haraguchi N, Mimori K, Matsumoto T, Inoue H, Yanaga K and Mori M. Clinicopathological and biological significance of mitotic centromere-associated kinesin overexpression in human gastric cancer. Br J Cancer 2007; 97: 543-549.

[28] Ishikawa K, Kamohara Y, Tanaka F, Haraguchi N, Mimori K, Inoue H and Mori M. Mitotic centromere-associated kinesin is a novel marker for prognosis and lymph node metastasis in colorectal cancer. Br J Cancer 2008; 98: 1824-1829.

[29] Shimo A, Tanikawa C, Nishidate T, Lin M, Matsuda K, Park J, Ueki T, Ohta T, Hirata K, Fukuda M, Nakamura Y and Katagiri T. Involvement of kinesin family member 2C/mitotic centromere-associated kinesin overexpression in mammary carcinogenesis. Cancer Sci 2008; 99: 62-70.

[30] Huang H, Feng J, Famulski J, Rattner JB, Liu ST, Kao GD, Muschel R, Chan GK and Yen TJ. Tripin/hSgo2 recruits MCAK to the inner centromere to correct defective kinetochore attachments. J Cell Biol 2007; 177: 413-424.

[31] Li C, Zhang Y, Yang Q, Ye F, Sun SY, Chen ES and Liou YC. NuSAP modulates the dynamics of kinetochore microtubules by attenuating MCAK depolymerisation activity. Sci Rep 2016; 6: 18773.

[32] Ritter A, Sanhaji M, Friemel A, Roth S, Rolle U, Louwen F and Yuan J. Functional analysis of phosphorylation of the mitotic centromere-associated kinesin by Aurora B kinase in human tumor cells. Cell Cycle 2015; 14: 3755-3767.

[33] Ha MJ, Yoon J, Moon E, Lee YM, Kim HJ and Kim W. Assignment of the kinesin family member 4 genes (KIF4A and KIF4B) to human chromosome bands Xq13.1 and 5q33.1 by in situ hybridization. Cytogenet Cell Genet 2000; 88: 41-42.
[34] Cho SY, Kim S, Kim G, Singh P and Kim DW. Integrative analysis of KIF4A, 9, 18A, and 23 and their clinical significance in low-grade glioma and glioblastoma. Sci Rep 2019; 9: 4599.
[35] Song X, Zhang T, Wang X, Liao X, Han C, Yang C, Su K, Cao W, Gong Y, Chen Z, Han Q and Li J. Distinct diagnostic and prognostic values of kinesin family member genes expression in patients with breast cancer. Med Sci Monit 2018; 24: 9442-9464.
[36] Xue D, Cheng P, Han M, Liu X, Xue L, Ye C, Wang K and Huang J. An integrated bioinformatical analysis to evaluate the role of KIF4A as a prognostic biomarker for breast cancer. Onco Targets Ther 2018; 11: 4755-4768.
[37] Pan LN, Zhang Y, Zhu CJ and Dong ZX. Kinesin KIF4A is associated with chemotherapeutic drug resistance by regulating intracellular trafficking of lung resistance-related protein. J Zhejiang Univ Sci B 2017; 18: 1046-1054.
[38] Shan L, Zhao M, Lu Y, Ning H, Yang S, Song Y, Chai W and Shi X. CENPE promotes lung adenocarcinoma proliferation and is directly regulated by FOXM1. Int J Oncol 2019; 55: 257-266.
[39] Liang Y, Ahmed M, Guo H, Soares F, Hua JT, Gao S, Lu C, Poon C, Han W, Langstein J, Ekram MB, Li B, Davicioni E, Takhar M, Erho N, Karnes RJ, Chadwick D, van der Kwast T, Boutros PC, Arrowsmith CH, Feng FY, Joshua AM, Zoubeidi A, Cai C and He HH. LSD1-mediated epigenetic reprogramming drives CENPE expression and prostate cancer progression. Cancer Res 2017; 77: 5479-5490.
[40] Valentine MT, Fordyce PM and Block SM. Eg5 steps it up! Cell Div 2006; 1: 31.
[41] Venere M, Horbinski C, Crish JF, Jin X, Vasanji A, Major J, Burrows AC, Chang C, Prokop J, Wu Q, Sims PA, Canoll P, Summers MK, Rosenfeld SS and Rich JN. The mitotic kinesin KIF11 is a driver of invasion, proliferation, and self-renewal in glioblastoma. Sci Transl Med 2015; 7: 304ra143.
[42] Liu X, Gong H and Huang K. Oncogenic role of kinesin proteins and targeting kinesin therapy. Cancer Sci 2013; 104: 651-656.
[43] Thériault BL, Pajovic S, Bernardini MQ, Shaw PA and Gallie BL. Kinesin family member 14: an independent prognostic marker and potential therapeutic target for ovarian cancer. Int J Cancer 2012; 130: 1844-1854.
[44] Abiatari I, DeOliveira T, Kerkadze V, Schwager C, Esposito I, Giese NA, Huber P, Bergman F, Abdollahi A, Friess H and Kleeff J. Consensus transcriptome signature of perineural invasion in pancreatic carcinoma. Mol Cancer Ther 2009; 8: 1494-1504.
[45] Corson TW, Huang A, Tsao MS and Gallie BL. KIF14 is a candidate oncogene in the 1q minimal region of genomic gain in multiple cancers. Oncogene 2005; 24: 4741-4753.
[46] Corson TW and Gallie BL. KIF14 mRNA expression is a predictor of grade and outcome in breast cancer. Int J Cancer 2006; 119: 1088-1094.
[47] Corson TW, Zhu CQ, Lau SK, Shepherd FA, Tsao MS and Gallie BL. KIF14 messenger RNA expression is independently prognostic for outcome in lung cancer. Clin Cancer Res 2007; 13: 3229-3234.
[48] Madhavan J, Coral K, Mallikarjuna K, Corson TW, Amit N, Khetan V, George R, Biswas J, Gallie BL and Kumaramanickavel G. High expression of KIF14 in retinoblastoma: association with older age at diagnosis. Invest Ophthalmol Vis Sci 2007; 48: 4901-6.
[49] Wu Y, Wang A, Zhu B, Huang J, Lu E, Xu H, Xia W, Dong G, Jiang F and Xu L. KIF18B promotes tumor progression through activating the Wnt/beta-catenin pathway in cervical cancer. Onco Targets Ther 2018; 11: 1707-1720.
[50] Itzel T, Scholz P, Maass T, Krupp M, Marquardt JU, Strand S, Becker D, Staib F, Binder H, Roessler S, Wang XW, Thorgeirsson S, Müller M, Galle PR and Teufel A. Translating bioinformatics in oncology: guilt-by-profiling analysis and identification of KIF18B and CDCA3 as novel driver genes in carcinogenesis. Bioinformatics 2015; 31: 216-224.
[51] Bayo J, Fiore EJ, Dominguez LM, Real A, Malvicini M, Rizzo M, Atorrasagasti C, García MG, Argemi J, Martinez ED and Mazzolini GD. A comprehensive study of epigenetic alterations in hepatocellular carcinoma identifies potential therapeutic targets. J Hepatol 2019; 71: 78-90.
[52] Shen T, Yang L, Zhang Z, Yu J, Dai L, Gao M, Shang Z and Niu Y. KIF20A affects the prognosis of bladder cancer by promoting the proliferation and metastasis of bladder cancer cells. Dis Markers 2019; 2019: 4863182.
[53] Li H, Zhang W, Sun X, Chen J, Li Y, Niu C, Xu B and Zhang Y. Overexpression of kinesin family member 20A is associated with unfavorable clinical outcome and tumor progression in epithelial ovarian cancer. Cancer Manag Res 2018; 10: 3433-3450.
[54] Zhao X, Zhou L, Li X, Ni J, Chen P, Ma R, Wu J and Feng J. Overexpression of KIF20A confers malignant phenotype of lung adenocarcinoma by promoting cell proliferation and inhibiting apoptosis. Cancer Med 2018; 7: 4678-4689.

[55] Jung YD, Cho JH, Park S, Kang M, Park SJ, Choi DH, Jeong M, Park KC, Yeom YI and Lee DC. Lactate activates the E2F pathway to promote cell motility by up-regulating microtubule modulating genes. Cancers (Basel) 2019; 11.
[56] Kato T, Wada H, Patel P, Hu H, Lee D, Ujiie H, Hirohashi K, Nakajima T, Sato M, Kaji M, Kaga K, Matsui Y, Tsao M and Yasufuku K. Overexpression of KIF23 predicts clinical outcome in primary lung cancer patients. Lung Cancer 2016; 92: 53-61.
[57] Kato T, Lee D, Wu L, Patel P, Young AJ, Wada H, Hu HP, Ujiie H, Kaji M, Kano S, Matsuge S, Domen H, Kaga K, Matsui Y, Kanno H, Hatanaka Y, Hatanaka KC, Matsuno Y, de Perrot M and Yasufuku K. Kinesin family members KIF11 and KIF23 as potential therapeutic targets in malignant pleural mesothelioma. Int J Oncol 2016; 49: 448-456.
[58] Li XL, Ji YM, Song R, Li XN and Guo LS. KIF23 promotes gastric cancer by stimulating cell proliferation. Dis Markers 2019; 2019: 9751923.

Table S1. Multivariate analysis of overall survival in 366 HCC specimens

	Hazard Ratio	95% CI	*P*
Sex	1.03	0.52-2.05	0.931
Age	1.72	0.95-3.09	0.056814
Weight	0.68	0.39-1.18	0.174
Stage	2.53	1.63-3.94	0.000*
KIF2C	1.27	1.13-1.43	0.000*

*represents statistically significant differences ($p < 0.05$).

Table S2. Multivariate analysis of overall survival in 366 HCC specimens

	Hazard Ratio	95% CI	*P*
Sex	1.05	0.52-2.11	0.888
Age	1.82	1.00-3.30	0.048*
Weight	0.62	0.35-1.18	0.097
Stage	2.53	1.63-1.09	0.000*
KIF4A	1.22	1.09-1.37	0.001*

*represents statistically significant differences ($p < 0.05$).

Table S3. Multivariate analysis of overall survival in 366 HCC specimens

	Hazard Ratio	95% CI	*P*
Sex	0.87	0.43-1.74	0.686
Age	1.87	1.04-3.38	0.038*
Weight	0.56	0.31-0.99	0.045*
Stage	2.55	1.64-3.96	0.000*
KIF10	1.31	1.14-1.50	0.000*

*represents statistically significant differences ($p < 0.05$).

Table S4. Multivariate analysis of overall survival in 366 HCC specimens

	Hazard Ratio	95% CI	*P*
Sex	0.97	0.49-1.94	0.936
Age	1.99	1.08-3.66	0.026*
Weight	0.61	0.35-1.07	0.083
Stage	2.55	1.64-3.97	0.000*
KIF11	1.32	1.13-1.54	0.001*

*represents statistically significant differences ($p < 0.05$).

Table S5. Multivariate analysis of overall survival in 366 HCC specimens

	Hazard Ratio	95% CI	*P*
Sex	0.92	0.46-1.87	0.827
Age	1.89	1.04-3.42	0.037*
Weight	0.58	0.33-1.03	0.064
Stage	2.70	1.75-4.17	0.000*
KIF14	1.21	1.06-1.39	0.006*

*represents statistically significant differences ($p < 0.05$).

Table S6. Multivariate analysis of overall survival in 366 HCC specimens

	Hazard Ratio	95% CI	*P*
Sex	0.91	0.45-1.83	0.787
Age	1.94	1.06-3.56	0.032*
Weight	0.63	0.36-1.12	0.113
Stage	2.66	1.72-4.12	0.000*
KIF18B	1.24	1.10-1.40	0.000*

*represents statistically significant differences ($p < 0.05$).

Table S7. Multivariate analysis of overall survival in 366 HCC specimens

	Hazard Ratio	95% CI	*P*
Sex	0.92	0.46-1.85	0.823
Age	2.03	1.10-3.74	0.024*
Weight	0.65	0.37-1.14	0.132
Stage	2.64	1.70-4.10	0.000*
KIF20A	1.34	1.17-1.54	0.000*

*represents statistically significant differences ($p < 0.05$).

Table S8. Multivariate analysis of overall survival in 366 HCC specimens

	Hazard Ratio	95% CI	*P*
Sex	0.95	0.47-1.90	0.877
Age	1.85	1.02-3.35	0.042*
Weight	0.63	0.36-1.11	0.111
Stage	2.61	1.68-4.05	0.000*
KIF23	1.20	1.07-1.36	0.002*

*represents statistically significant differences ($p < 0.05$).

Table S9. KEGG analyses of the pathways of the eight-KIF gene prediction model

NAME	SIZE	ES	NES	NOM *p*-val	FDR q-val	FWER *p*-val
KEGG_CELL_CYCLE	118	0.713	2.360	0.000	0.000	0.000
KEGG_BASE_EXCISION_REPAIR	33	0.748	2.243	0.000	0.001	0.002
KEGG_OOCYTE_MEIOSIS	112	0.559	2.194	0.000	0.001	0.003
KEGG_HOMOLOGOUS_RECOMBINATION	26	0.796	2.133	0.000	0.003	0.007
KEGG_PROGESTERONE_MEDIATED_OOCYTE_MATURATION	85	0.530	2.006	0.000	0.009	0.039
KEGG_DNA_REPLICATION	36	0.821	1.996	0.000	0.010	0.045
KEGG_MISMATCH_REPAIR	23	0.763	1.951	0.000	0.016	0.071
KEGG_P53_SIGNALING_PATHWAY	67	0.489	1.935	0.000	0.018	0.086
KEGG_BLADDER_CANCER	42	0.539	1.888	0.000	0.026	0.122
KEGG_PURINE_METABOLISM	158	0.390	1.705	0.000	0.105	0.477
KEGG_COMPLEMENT_AND_COAGULATION_CASCADES	68	-0.825	-2.303	0.000	0.001	0.001
KEGG_TRYPTOPHAN_METABOLISM	40	-0.732	-2.127	0.000	0.007	0.008
KEGG_FATTY_ACID_METABOLISM	40	-0.816	-1.996	0.000	0.018	0.047
KEGG_LINOLEIC_ACID_METABOLISM	28	-0.645	-1.959	0.000	0.018	0.073
KEGG_DRUG_METABOLISM_CYTOCHROME_P450	71	-0.692	-2.102	0.002	0.008	0.016
KEGG_SPLICEOSOME	114	0.654	2.053	0.002	0.007	0.024
KEGG_PRIMARY_BILE_ACID_BIOSYNTHESIS	16	-0.810	-1.825	0.002	0.030	0.223
KEGG_PROPANOATE_METABOLISM	32	-0.755	-1.915	0.002	0.021	0.109
KEGG_PYRIMIDINE_METABOLISM	98	0.479	1.808	0.002	0.055	0.264
KEGG_HISTIDINE_METABOLISM	29	-0.617	-1.886	0.004	0.023	0.148
KEGG_PEROXISOME	77	-0.673	-2.006	0.004	0.021	0.040
KEGG_VALINE_LEUCINE_AND_ISOLEUCINE_DEGRADATION	44	-0.796	-1.983	0.006	0.017	0.053
KEGG_TYROSINE_METABOLISM	42	-0.569	-1.839	0.006	0.030	0.202
KEGG_BUTANOATE_METABOLISM	34	-0.711	-1.924	0.006	0.021	0.098
KEGG_BETA_ALANINE_METABOLISM	22	-0.703	-1.837	0.008	0.029	0.205
KEGG_PPAR_SIGNALING_PATHWAY	69	-0.579	-1.879	0.008	0.023	0.158
KEGG_NUCLEOTIDE_EXCISION_REPAIR	44	0.569	1.823	0.008	0.052	0.237
KEGG_NON_SMALL_CELL_LUNG_CANCER	54	0.457	1.703	0.008	0.099	0.481
KEGG_PATHOGENIC_ESCHERICHIA_COLI_INFECTION	53	0.517	1.716	0.010	0.103	0.458
KEGG_UBIQUITIN_MEDIATED_PROTEOLYSIS	134	0.392	1.656	0.010	0.134	0.591
KEGG_RETINOL_METABOLISM	63	-0.662	-1.961	0.010	0.020	0.073

NOM *p*-val, nominal *p* value.

Table S10. Oncogenic signature analyses of the gene sets associated with the eight-KIF gene prediction model

NAME	SIZE	ES	NES	NOM *p*-val	FDR q-val	FWER *p*-val
RPS14_DN.V1_DN	185	0.563	2.325	0.000	0.000	0.000
CSR_LATE_UP.V1_UP	170	0.622	2.296	0.000	0.000	0.000
PRC2_EZH2_UP.V1_DN	188	0.562	2.272	0.000	0.000	0.000
RB_P107_DN.V1_UP	136	0.675	2.264	0.000	0.000	0.000
E2F1_UP.V1_UP	185	0.557	2.243	0.000	0.000	0.000
GCNP_SHH_UP_LATE.V1_UP	177	0.553	2.178	0.000	0.000	0.000
PRC2_EED_UP.V1_DN	191	0.518	2.115	0.000	0.000	0.001
RB_DN.V1_UP	131	0.501	2.068	0.000	0.000	0.003
GCNP_SHH_UP_EARLY.V1_UP	171	0.503	2.030	0.000	0.000	0.004
HOXA9_DN.V1_DN	186	0.466	1.983	0.000	0.001	0.009

SRC_UP.V1_DN	165	0.430	1.844	0.000	0.005	0.059
E2F3_UP.V1_UP	187	0.430	1.816	0.002	0.006	0.075
VEGF_A_UP.V1_DN	189	0.485	1.817	0.002	0.006	0.075
RB_P130_DN.V1_UP	128	0.424	1.657	0.008	0.032	0.293
BMI1_DN_MEL18_DN.V1_DN	146	-0.443	-1.883	0.000	0.051	0.038
MEL18_DN.V1_DN	148	-0.445	-1.849	0.000	0.036	0.058
AKT_UP.V1_DN	186	-0.423	-1.840	0.000	0.026	0.063
BMI1_DN.V1_DN	141	-0.411	-1.751	0.000	0.056	0.146
PKCA_DN.V1_UP	167	-0.405	-1.719	0.000	0.065	0.187

NOM *p*-val, nominal *p* value.

Table S11. The primer sequences used in this study

Name	Sequence 5'-3'
KIF2C-forward	CGCGTTTCTCTTCCTTGCTG
KIF2C-reverse	TCTTGATAGCGAGACCGGGA
KIF4A-forward	TAACCGAGGCCTCCTATGCT
KIF4A-reverse	CTCTGTAGGGCACAAAGCCA
KIF10-forward	GACCGACAGAACCACCAAGT
KIF10-reverse	TCAGGCTTTCCGTAAGGTGC
KIF11-forward	ATCAATTGGCGGGGTTCCAT
KIF11-reverse	CTGGGCTCGCAGAGGTAATC
KIF14-forward	ATTCAAATTGCGGCCTTCTGG
KIF14-reverse	GCCTGTAGGGAAAGCGTCC
KIF18B-forward	GTGTGGGTACTGCTGTCTGT
KIF18B-reverse	CTGTCCTCCACTGCCATCAC
KIF20A-forward	TCGGCGACTAGGTGTGAGTA
KIF20A-reverse	ACGACATCGTCATCGGACAG
KIF23-forward	CCATAAAACCCAAACCTCCACA
KIF23-reverse	ACGTCTCTTTTTCTGGCCTCT
β-actin-forward	TTGTTACAGGAAGTCCCTTGCC
β-actin-reverse	ATGCTATCACCTCCCCTGTGTG

Table S12. The siRNA sequences used in this study

Name	Sequence
KIF2C-siRNA1	GCAAGAAUUGGCCAAGAAATT
	UUUCUUGGCCAAUUCUUGCTT
KIF2C-siRNA2	GCUGAGGGACUCCUUCAUUTT
	AAUGAAGGAGUCCCUCAGCTT
KIF4A-siRNA1	GGAAUGAGGUUGUGAUCUUTT
	AAGAUCACAACCUCAUUCCTT
KIF4A-siRNA2	GGUCCAGACUACUACUCUATT
	UAGAGUAGUAGUCUGGACCTT
KIF10-siRNA1	GCUACUAAAUCAGGAGAAUTT
	AUUCUCCUGAUUUAGUAGCTT
KIF10-siRNA2	CCAGUUGACUAAGAAACUUTT
	AAGUUUCUUAGUCAACUGGTT

KIF11-siRNA1	GCCCAUUCAAUAGUAGAAUTT
	AUUCUACUAUUGAAUGGGCTT
KIF11-siRNA2	GGUGUGGAUUGUUCAUCAATT
	UUGAUGAACAAUCCACACCTT
KIF14-siRNA1	GCAGUACGCGUAAGACCUUTT
	AAGGUCUUACGCGUACUGCTT
KIF14-siRNA2	GCAAGAAUUCUGGAAGCUUTT
	AAGCUUCCAGAAUUCUUGCTT
KIF18B-siRNA1	GCUACCAGGAGGUGUAUAATT
	UUAUACACCUCCUGGUAGCTT
KIF18B-siRNA2	GCAAAGACCUGACGUUUGUTT
	ACAAACGUCAGGUCUUUGCTT
KIF20A-siRNA1	GCAUCUACCUAUGAUGAAATT
	UUUCAUCAUAGGUAGAUGCTT
KIF20A-siRNA2	CCACUUGUGAUGACAUCUUTT
	AAGAUGUCAUCACAAGUGGTT
KIF23-siRNA1	GGUCCCAAACGAACCUUAATT
	UUAAGGUUCGUUUGGGACCTT
KIF23-siRNA2	GCUAUUGUUACCGAACCUATT
	UAGGUUCGGUAACAAUAGCTT

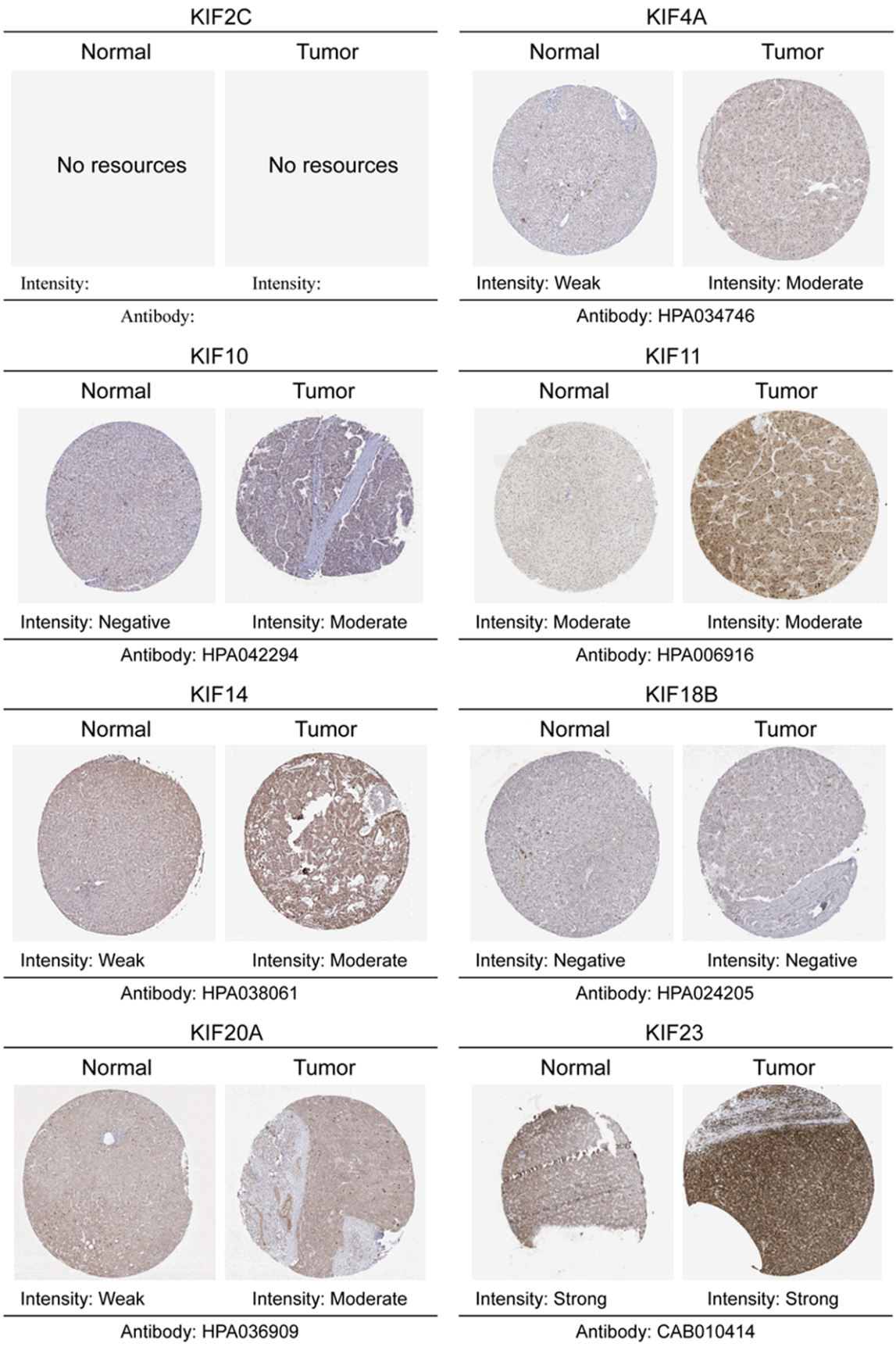

Figure S1. Representative immunohistochemistry images of distinct KIF superfamily members in HCC tissues and normal liver tissues (images were obtained from The Human Protein Atlas).